A hidden succession revealed: Cretaceous and Paleocene sediments and a native-iron-bearing lava flow in cores near Qullissat, Disko, West Greenland

Lotte Melchior Larsen*[1], Gunver Krarup Pedersen[1], Henrik Nøhr-Hansen[1], Asger Ken Pedersen[1,2], Jørgen A. Bojesen-Koefoed[1], Erik Vest Sørensen[1], Sofie Lindström[1,3]

[1]Geological Survey of Denmark and Greenland (GEUS), Copenhagen, Denmark, [2]Natural History Museum of Denmark, Copenhagen, Denmark, [3]Department of Geosciences and Natural Resource Management, Copenhagen University, Copenhagen, Denmark

Abstract

Over long stretches of the north-east coast of Qeqertarsuaq (Disko), the sediments in the Nuussuaq Basin and their relations to the volcanic rocks are concealed beneath numerous landslides. Two cores south of Qullissat drilled by Falconbridge Ltd in 1994, targeting a native-iron-bearing igneous body assumed to be a sill, present well-preserved sections through the hidden succession. We have dated the sediments in the cores palynologically. The lower part comprises 115 m of deltaic deposits, including coal seams, of the Cretaceous Atane Formation, Qilakitsoq Member (late Turonian to early Coniacian age), which has not been recorded on Disko before. The two cores and five short coastal cliff sections are mutually correlatable and correlate further to the coal seams earlier mined at Qullissat; the coals are hereby dated for the first time. The Cretaceous rocks are overlain by 15 m of marine deposits, mainly mudstones, of the Danian Eqalulik Formation, with a hiatus of c. 24 million years. The igneous body of native-iron-bearing basaltic andesite has a thick, red-oxidised, vesiculated and brecciated top zone and is interpreted as a subaerial lava flow belonging to the Asuk Member of the Vaigat Formation. The flow has run perhaps up to 20 km from the eruption site to the sea, where it ponded and attained a thickness of 138 m, the thickest lava flow in the West Greenland Basalt Group. The flow is overlain by 22 m of non-marine sandstones and mudstones of the Atanikerluk Formation. The core correlation indicates the existence of a fault with c. 90 m vertical displacement between the two drill sites. The structural relations of the various parts of the Atane Formation along the north-east coast of Disko necessitate the assumption of another hidden, prevolcanic fault south of Qullissaaqqat.

1 Introduction

The Nuussuaq Basin in West Greenland contains exposed sedimentary rocks of Cretaceous to Palaeogene age overlain and intruded by volcanic rocks of Palaeogene age. The basin is one of the most intensely investigated regions in Greenland, and coal deposits in the sediments and mineralisations of iron, nickel, copper and platinum-group elements in the volcanic rocks have been explored and exploited for more than hundred years. Nowhere in the basin have these activities been more intense than in the northern part of Qeqertarsuaq (Disko), particularly in the Qullissat area where a coal mine and an associated town (Qullissat) with more than thousand inhabitants were situated (Fig. 1). The geological relations in the Nuussuaq Basin are generally well mapped and understood (e.g. Clarke & Pedersen 1976; Dam *et al*. 2009; Larsen *et al*. 2016; Pedersen *et al*. 2017, 2018; Dam & Sønderholm 2021; Larsen & Larsen 2022). However, the north-east coast of Disko, including the area around Qullissat, has been difficult to examine geologically because of numerous landslides (e.g. Svennevig *et al*. 2023). Here, Cretaceous strata with coal seams of the Atane Formation are well exposed in the coastal cliffs up to *c.* 50 m altitude, and the Paleocene volcanic succession of the Vaigat and
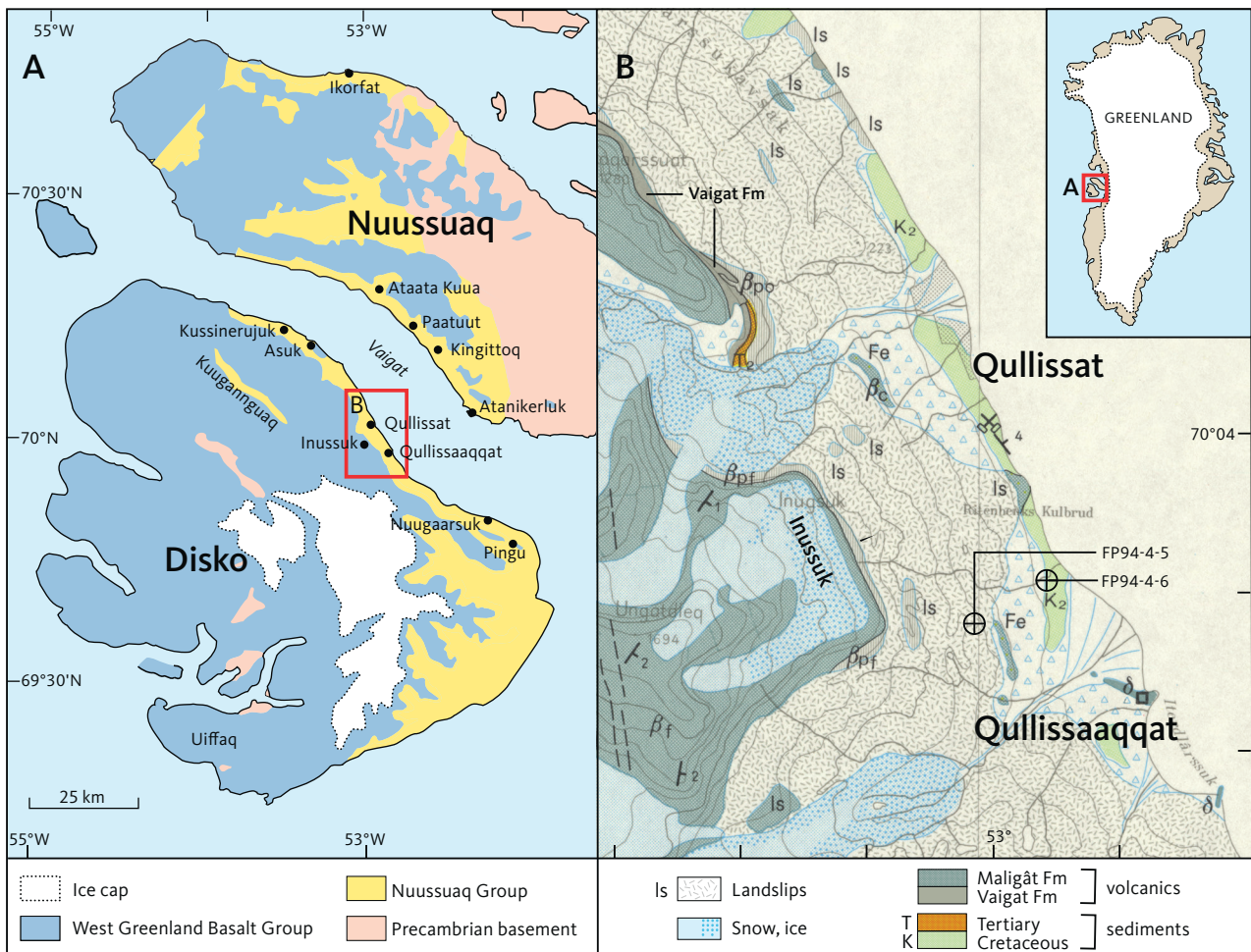
Fig. 1 Geological maps of parts of the Nuussuaq Basin. **A**: Overview map of Disko and Nuussuaq, with names mentioned in the text and the position of Fig. 1B indicated. **B**: Map of the area around Qullissat and Qullissaaqqat, with boreholes FP94-4-5 and FP94-4-6 indicated. Two exposures of the iron-bearing igneous body studied here are labelled 'Fe'. Other labels are part of the geological divisions on the map. Excerpt from the geological map 1:100 000 Qutdligssat (old spelling, Rosenkrantz *et al*. 1976), reproduced to scale, i.e. 1 cm = 1 km.

Maligât Formations is excellently exposed in the steep mountain slopes above *c*. 700 m altitude. However, the intervening interval at *c*. 50–700 m altitude is dominated by landslides, and the rocks are extensively covered by talus and vegetation (Figs 1 and 2). Therefore, the lithostratigraphy of the Cretaceous and Paleocene sedimentary deposits and the relations between the sedimentary and volcanic rocks are poorly known over long stretches of the north-east coast of Disko. Even the age of the mined coal seams has not been well established.

The occurrences of volcanic rocks with native iron on Disko are world-famous (Pedersen *et al*. 2017, 2018 and numerous references therein) and have been repeatedly explored by mining companies (see next section). A native-iron- and sulphide-bearing, sill-like igneous body occurs in the sediments between Qullissat and Qullissaaqqat but is poorly exposed and partly displaced by landslides (Fig. 1B). This body has attracted mining companies that assumed an analogy to iron-bearing igneous rocks in the Noril'sk region in Siberia (Lightfoot &

Hawkesworth 1997, their figs 14 and 15), where a crucial mechanism is considered to be metal and sulphide precipitation during magma flowage through subsurface intrusions (sills). In 1993 and 1994, the mining company Falconbridge Ltd. drilled five boreholes targeting the supposed sill; most were short due to technical difficulties, but the two cores FP94-4-5 and FP94-4-6 together constitute a long section of excellent quality through Cretaceous and Palaeogene sedimentary strata as well as the complete igneous body (Olshefsky & Jerome 1994; Olshefsky *et al*. 1995; Lode *et al*. 2021).

This paper presents the results of a study of the two cores, which represent the poorly known stratigraphic interval concealed by landslides. The cores have enabled us to place constraints on the stratigraphy, age and structure of the Cretaceous and Paleocene sedimentary strata in north-eastern Disko; they also show that the native-iron-bearing igneous body is not a sill but a subaerial lava flow, which we assign to the volcanic Asuk Member of the Vaigat Formation.
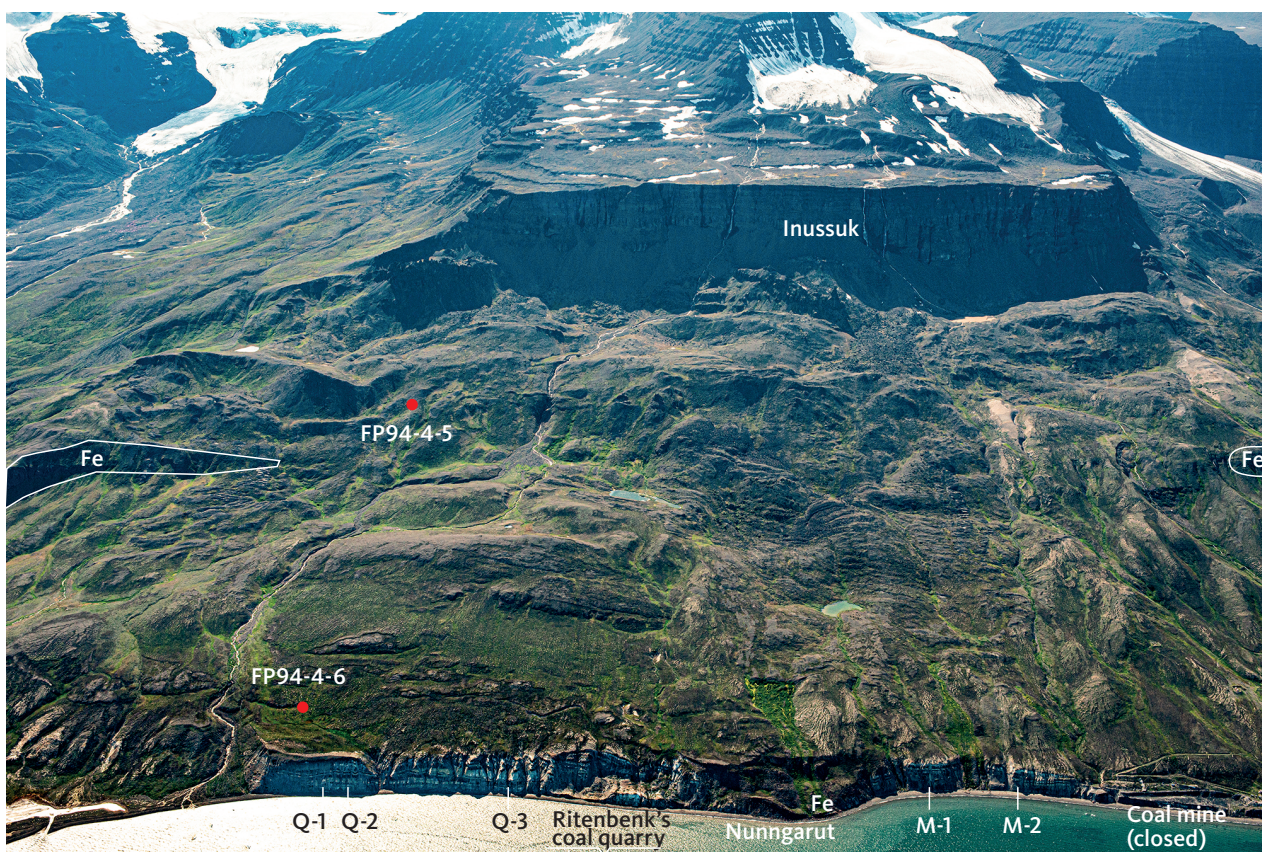
Fig. 2 Oblique aerial photograph of the coastal area of Disko between the closed coal mine (at right) and Qullissaaqqat (immediately left of the picture). Ritenbenk's old coal quarry is clearly seen from the air; seen on the ground it is inconspicuous. The positions of boreholes FP94-4-5 and FP94-4-6 and coastal sections Q-1, Q-2, Q3, M-1 and M-2 are indicated. Exposures of the Nunngarut igneous body (Fe) *in situ* are annotated with white lines to the right and left; a third exposure is seen in a landslide at the coast at Nunngarut. The height of the coastal cliffs is around 50 m, and the height of the plateau top of the Inussuk mountain is around 900 m. Note the tumbled and landslipped surface and lack of exposures between Inussuk and the coastal cliffs. Compare Fig. 3. Photo: Kristian Svennevig 2019.

2 History

In 1871 and 1872, K.J.V. Steenstrup was sent to Greenland with instructions to investigate the occurrence of native iron at Uiffaq in south-western Disko and at the same time to collect information on the occurrences of coal seams in the region. The second task brought him to the north-east coast of Disko, where several coal seams in the Atane Formation are intermittently exposed in the coastal cliffs between Qullissat and Qullissaaqqat (Gamle Qutdligssat) about 3 km south-east of Qullissat (Figs 1 and 2). The coal had been quarried since the 1770s near Qullissaaqqat ('Ritenbenk's coal quarry') for local use in the settlements in the Qeqertarsuup Tunua (Disko Bugt) region (Schiener 1976; Shekhar *et al*. 1982), and the Danish authorities wanted to increase the utilisation of the coal in West Greenland. Steenstrup (1874) published a description and a drawn section of the coal-bearing sediments in the coastal cliffs between the coal quarry and the alluvial fan where the Qullissat town later was built. The coal was mined at Qullissat between 1924 and 1972, when the mine was closed and the town abandoned (Schiener 1976).

Steenstrup also discovered a native-iron-bearing lava flow at Asuk 19 km north-west of Qullissat, the first iron occurrence found outside the Uiffaq locality. At Uiffaq, the origin of the iron, whether meteoritic or telluric, was disputed, and the Asuk locality has become famous because it proved beyond doubt that the iron is of telluric origin (Steenstrup 1875, 1877, 1882). Steenstrup also found the igneous body, which is described in the present work, and sampled it in a landslide at Nunngarut (Figs 2 and 3); he noted that it was graphite-bearing and only later found that it also carries native iron and closely resembles the iron-bearing rock at Asuk (Steenstrup 1900, p. 268). More recently, exploration for nickel, copper and precious metals in the volcanic rocks was carried out by the mining companies Kryolitselskabet Øresund A/S in the 1950–1960s, Greenex Ltd. in the 1980s and Falconbridge Ltd. in the 1990s.

3 Geological setting

The Nuussuaq Basin is a rift basin that extends for *c*. 400 km along the coast of West Greenland (Chalmers *et al*. 1999; Chalmers & Pulvertaft 2001; Hopper *et al*.
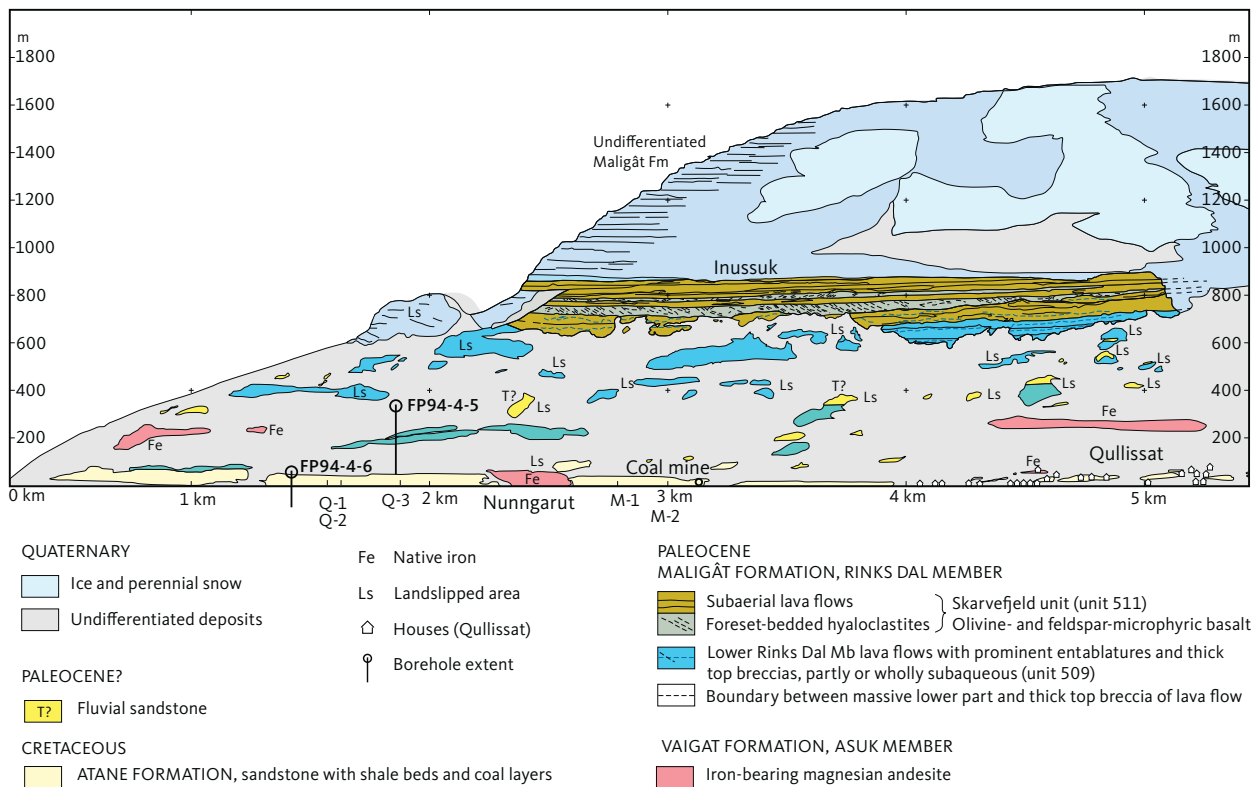
Fig. 3 Photogrammetrically measured and interpreted section along the coast of Disko between Qullissat (at right) and Qullissaaqqat (immediately left of the section). Exposures of the iron-bearing Nunngarut igneous body are red. The vertical extents of boreholes FP94-4-5 and FP94-4-6 are indicated. Compare Fig. 2, but note that the perspectives are very different because the section possesses no single point of view. Modified from fig. 48 in Pedersen *et al*. (2018) or fig. 161 in Pedersen *et al*. (2017).

2016; Dam & Sønderholm 2021). In the Disko–Nuussuaq area (Fig. 1A), the sedimentary strata are of Albian to Paleocene age and constitute the Nuussuaq Group (Fig. 4; Dam *et al*. 2009; Pedersen & Nøhr-Hansen 2014; Nøhr-Hansen *et al*. 2016; Pedersen *et al*. 2023). The structural development includes an early rift phase, a subsidence phase, a late rift phase and a drift phase. These four phases comprise eight tectonostratigraphic sequences (TSS1–TSS8) described and interpreted by Dam & Sønderholm (2021, their fig. 3), see Fig. 4.

TSS1 (Albian) comprises fluvial and lacustrine deposits of the Kome and Slibestensfjeldet Formations in northern Nuussuaq.

During the deposition of TSS2 to TSS4 (late Albian to earliest Campanian), a huge delta system built out from the south-east, and sedimentary material was transported towards north-west, west and south-west across a delta plain with coal swamps and shallow lakes (Pedersen & Pulvertaft 1992). The fluvial system may have had a drainage area that covered large parts of 'the interior' of Greenland (Olsen 1993; Dam *et al*. 2020). The delta front prograded repeatedly towards the north, north-west and west (Dam *et al*. 2009; Dam & Sønderholm 2021). The fluvial, delta plain, shoreface and delta front deposits constitute the Atane Formation, which is seen in outcrops in Disko and in southern, central and

northern Nuussuaq. TSS4 also includes the lower part of the marine Itilli Formation, i.e. the Kussinerujuk Member in northern Disko from Asuk and westwards (Dam *et al*. 2009).

The Atane Formation is overlain by submarine slope, fan and channel deposits in northern and central Nuussuaq. They constitute the Aaffarsuaq Member of the Itilli Formation (Dam *et al*. 2009) and belong to TSS5 (Campanian to early Maastrichtian). In central Nuussuaq, the base of TSS5 is an angular unconformity (Dam *et al*. 2000). This early Campanian unconformity is recognised offshore in regional geophysical datasets (Gregersen *et al*. 2013, 2019, 2022).

TSS6 comprises the Kangilia Formation (latest Maastrichtian and Danian age, Fig. 4), which consists of a thick conglomerate unit interpreted as a turbidity channel deposit, overlain by deep-water marine turbiditic mudstones (figs 76, 95 in Dam *et al*. 2009). The formation is exposed in northern and western Nuussuaq. At the south coast of Nuussuaq (Ataata Kuua), the Kangilia Formation fills a submarine canyon (Dam *et al*. 2009, figs 14, 15, 91).

TSS7 (Danian) comprises the complex fill of incised valleys of fluvial and submarine origin. Thick fluvial and lacustrine successions of the Quikavsak Formation truncate the Atane and Kangilia Formations in southern
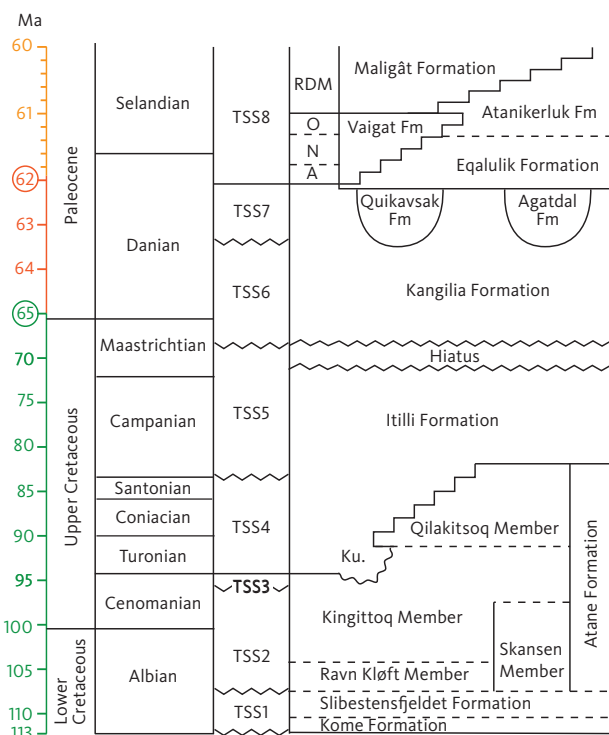
Fig. 4 Stratigraphy and age of the sedimentary and volcanic formations of the Nuussuaq Basin on Disko and Nuussuaq. On the age scale to the left, rings around two numbers and change of colours indicate changes in the scale. TSS-1 to TSS-8 are tectonostratigrahic sequences (Dam & Sønderholm 2021). Ku.: Kussinerujuk Member. Members of the volcanic formations are A: Anaanaa Member; N: Naujánguit Member; O: Ordlingassoq Member; RDM: Rinks Dal Member.

Nuussuaq, while thick, marine turbiditic sandstones and conglomerates of the Agatdal Formation overlie the Kangilia Formation in central Nuussuaq (Dam *et al*. 2009, figs 109, 114). The dramatic changes in water depth from the marine deep-water Kangilia Formation to the incised fluvial valleys (Quikavsak Formation) and the return to deep-water conditions (Eqalulik Formation) at the south coast of Nuussuaq indicate a Danian uplift presumably caused by arrival of the Proto-Icelandic Mantle plume (Dam & Nøhr-Hansen 2001; Dam & Sønderholm 2021).

TSS8 (Danian to Selandian) comprises both synvolcanic sediments, which drape the prevolcanic deposits, and volcanic rocks. The Eqalulik Formation in the north and west consists of tuffaceous mudstones deposited in a deep marine embayment bounded to the west by the advancing volcanic front. The Atanikerluk Formation, in the east and south, consists of siliciclastic sediments deposited from the east in lacustrine and fluvial environments. The lacustrine mudstones include thin layers of volcanic ash (Pedersen *et al*. 1998; Dam *et al*. 2009).

The volcanic rocks of TSS8 in the Disko – Nuussuaq area comprise the Vaigat and Maligât Formations (Fig. 4). Eruption of the Vaigat Formation magmas started in western Nuussuaq and expanded eastwards and southwards to cover successively larger areas with hyaloclastites and overlying associated subaerial lava flows (Pedersen *et al*. 2017). Three major volcanic episodes gave rise to the three main members: the Anaanaa, Naujánguit and Ordlingassoq Members (Fig. 4). The eastward progradation of the hyaloclastites of the Anaanaa and Naujánguit Members into the marine embayment gradually narrowed the connection to the open sea north of Nuussuaq. The connection was finally blocked at the end of the second volcanic episode, leaving a brackish and eventually freshwater lake that covered large areas of south-central to south-eastern Nuussuaq and north-eastern Disko. In this lake, the Atanikerluk Formation was deposited (Pedersen *et al*. 1996; Pedersen *et al*. 1998). Hyaloclastites of the third volcanic episode continued the eastward progradation into the lake and reduced its extent and water depth. The lake expanded westwards during the pause between the Vaigat and Maligât formations, and when the Maligât Formation started to erupt from centres in south-western Disko, a new lake covered eastern Disko and southernmost Nuussuaq. This lake was gradually filled with more sediments of the Atanikerluk Formation (Assoq Member) and hyaloclastites and subaqueous lava flows of the Maligât Formation (Dam *et al.* 2009; Pedersen *et al.* 2018, fig. 16).

4 Geology of the formations represented in the drill cores

4.1 Sedimentary rocks

4.1.1 Atane Formation
The Atane Formation comprises fluvial and deltaic deposits of late Albian to latest Santonian–earliest Campanian age in Nuussuaq and Disko (Fig. 4). The lower boundary is exposed at the north coast of Nuussuaq. In Disko, the contact between weathered basement and fluvial deposits is recorded in borehole FP93-3-1 in the Kuugannguaq valley west of Qullissat (Dam *et al.* 2009, fig. 19). The upper boundary of the Atane Formation consists of erosional unconformities overlain by the Aaffarsuaq Member of the Itilli Formation (central Nuussuaq), the Quikavsak Formation (south coast of Nuussuaq), the Kussinerujuk Member of the Itilli Formation (north coast of Disko) and the Eqalulik and Atanikerluk Formations (northern and eastern Disko and south-eastern Nuussuaq). The Atane Formation comprises four members, the distribution of which is shown in Fig. 5.

The Ravn Kløft Member (late Albian age) is known only from the north coast of Nuussuaq (Fig. 5). It is interpreted as estuarine and is overlain by the deltaic Kingittoq Member (Midtgaard 1996; Dam *et al.* 2009; Pedersen & Nøhr-Hansen 2014; Pedersen *et al.* 2023).
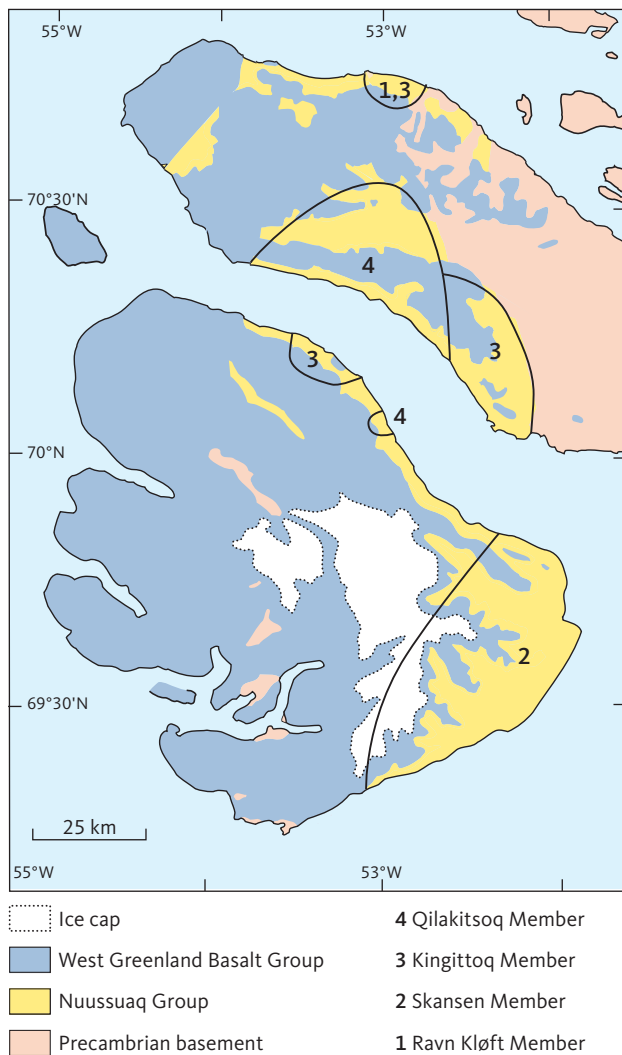
Fig. 5 Map showing schematically the known extents of the four members of the Atane Formation of the Nuussuaq Group. The lines do not indicate member boundaries but knowledge limitations: members can only be assigned in the areas with numbers 1 to 4. The Atane Formation is not present in western and northern Nuussuaq, except in the area labelled 1 and 3.

The Skansen Member (late Albian to mid-Cenomanian age) is exposed in eastern Disko (Fig. 5). It is characterised by thick fluvial sandstones interbedded with thinner units of mudstone and thin coal beds, interpreted as flood-plain deposits (Koppelhus & Pedersen 1993). The member is exposed on the north coast of Disko from Pingu and *c.* 10 km westwards to Nuugaarsuk. From Nuugaarsuk and north-westwards to Qullissaaqqat, the coastal cliffs are strongly affected by landslides, and the Cretaceous deposits form loose, sand-dominated scree slopes, which have not been closely investigated. The sedimentological model predicts that the Skansen Member is replaced basinwards (north-westwards) by delta deposits of the same age, referred to the Kingittoq Member (Fig. 4). A very long hiatus separates the Skansen Member from the overlying synvolcanic, fluvial

sediments of the Paleocene Akunneq Member of the Atanikerluk Formation (Pedersen *et al.* 1998; Dam *et al.* 2009, fig. 16).

The Kingittoq Member represents stacked deltaic deposits exposed at the north coast of Nuussuaq east of Ikorfat, at the south coast of Nuussuaq from Atanikerluk to Kingittoq and at the north coast of Disko from east of Asuk ('Asuk East') and westwards to Kussinerujuk (Fig. 4). Between Asuk East and Kussinerujuk, the erosional unconformity TSS3 forms the boundary between the Kingittoq Member and the overlying Kussinerujuk Member (Itilli Formation) deposited in the early part of TSS4 (Dam *et al.* 2009; Fig. 5). The Kingittoq Member ranges in age from late Albian at Asuk, Atanikerluk and east of Ikorfat to middle Turonian at Kingittoq (Pedersen & Nøhr-Hansen 2014; Pedersen *et al.* 2023). Marine dinoflagellate cysts are scarce in the older part of the member but more frequent in its younger part. A similar pattern is known from the Baffin Bay (Nøhr-Hansen *et al.* 2021).

The Qilakitsoq Member represents stacked deltaic deposits in central Nuussuaq and at the south coast from Paatuut and westwards (Fig. 5). Many sections in central Nuussuaq show thick delta front deposits, wave-generated sedimentary structures are common and transgressive shoreface sandstones are well developed. The member is of early Coniacian to latest Santonian age in the borehole GGU 247801 and adjacent outcrops at Ataata Kuua on the south coast of Nuussuaq. The borehole did not reach a change in lithology that could be interpreted as the boundary to the older Kingittoq Member. Locally, the Qilakitsoq Member is of earliest Campanian age (Dam *et al.* 2000; Pedersen & Nøhr-Hansen 2014).

The Qilakitsoq Member has not previously been documented from Disko, although a fluvial sandstone of latest Cenomanian age overlies the Kussinerujuk Member at Asuk East. It was tentatively correlated to the Qilakitsoq Member (Pedersen & Nøhr-Hansen 2014), mostly because of its position above the Kussinerujuk Member.

4.1.1.1 Depositional history. The Atane Formation extends over distances of 150 km N–S and 60 km E–W. It represents deposits from the late Albian to the earliest Campanian (about 20–25 million years) and ranges from fluvial channel sandstones (Skansen Member) and complex, estuarine deposits (Ravn Kløft Member) to stacked delta deposits of the Kingittoq and Qilakitsoq Members. In the eastern part of the Nuussuaq Basin, the non-marine delta facies are dominant, while a stronger marine influence is observed in the western outcrops, especially in the Qilakitsoq Member. The lithostratigraphic overview of Dam *et al.* (2009, fig. 16) shows that a hiatus between the Cretaceous and the Palaeogene

sedimentary formations has the longest duration close to the basin boundary fault (eastern Disko and eastern Nuussuaq), whereas the succession in western Nuussuaq is almost continuous. A succession ranging from the lower Turonian to the upper Coniacian, such as that in cores FP94-4-5 and FP94-4-6, has not previously been documented in the Atane Formation (e.g. Pedersen & Nøhr-Hansen 2014, fig. 16).

4.1.2 Eqalulik Formation

This formation comprises dark grey to black, marine, synvolcanic mudstones with layers of volcanic ash (Dam *et al*. 2009). It is commonly poorly exposed due to talus deposits from steep cliffs of the overlying hyaloclastite breccias. Lateral correlations are rarely possible, except for a distinctive and widespread layer of graphite andesite tuff erupted from the Ilugissoq volcano of the Asuk Member of the Vaigat Formation in central Nuussuaq (Fig. 6; A.K. Pedersen & Larsen 2006; Pedersen *et al*. 2017). Dinoflagellate cysts in the Eqalulik Formation indicate a late Danian–early Selandian age (Nøhr-Hansen *et al*. 2002), which is consistent with radiometric ages of the Vaigat Formation (Storey *et al*. 1998). The Eqalulik Formation was deposited during a period of rapid subsidence, at least partly due to loading by the volcanic rocks; water depths of up to *c*. 600 m are demonstrated by the height of hyaloclastite foresets (Pedersen *et al*. 2017, figs 85, 87). Along the

Fig. 6 Map showing the distribution of the individual units of the Asuk Member. **CE**: Inferred central eruption area for the Asuk Member on Disko. The large, light grey circular area is the extent of the graphite andesite tuff layer erupted from the Ilugissoq volcano. The green areas show exposures of the Vaigat Formation, and the green lines are the eastern and south-eastern depositional boundaries of the large Naujánguit and Ordlingassoq Members of the Vaigat Formation. Modified from A.K. Pedersen *et al*. (2017, fig 10).

north-east coast of Disko, the eastern delimitation of the formation is uncertain because it is almost totally unexposed.

4.1.3 Atanikerluk Formation

The synvolcanic, lacustrine sandstones and mudstones in eastern Disko and south-eastern Nuussuaq constitute the Atanikerluk Formation (Koch 1959; Pedersen *et al*. 1998; Dam *et al.* 2009, figs 127–131). The formation comprises fluvial sandstones (the Akunneq Member) and lacustrine mudstones grading up into sandstones: the Naujât, Pingu, Umiussat and Assoq Members. Marine dinoflagellate cysts occur locally in the Assoq Member in southern Disko, which suggests intermittent contacts between the lake and marine waters to the south. The Atanikerluk Formation is bounded to the west by the Vaigat Formation (Ordlingassoq Member) and the Maligât Formation (Lower Rinks Dal Member). Its extent to the east and south is unknown, and it is possible that the lake was bounded to the east by the basin boundary fault (Pedersen *et al*. 2018, fig. 16).

4.2 Igneous rocks

4.2.1 Vaigat Formation

The volcanic rocks of the Vaigat Formation consist mainly of picrites, i.e. relatively primitive, magnesium-rich rocks that were erupted directly from the melt accumulation areas in the asthenospheric mantle. Particularly during the second volcanic episode, some magma batches stalled in the crust and became contaminated with carbon-bearing sediments before eruption. Such crustally contaminated rocks range from magnesium-poor picrites through basalts and magnesian basaltic andesites to magnesian andesites and now form five separate, minor members intercalated with the major, uncontaminated members (Pedersen *et al*. 2017). The uncontaminated picrites never reached as far east as the Qullissat area; those of the second volcanic episode (Naujánguit Member) stopped *c*. 10 km north-west of Qullissat, whereas those of the third volcanic episode (Ordlingassoq Member) stopped just above the site of the town (Fig. 6). Only the basalt flows of the Maligât Formation later overran the whole area (Fig. 3).

4.2.1.1 Asuk Member. The Asuk Member contains the most crustally contaminated rocks in the Vaigat Formation, with up to 40% sediment component, and is famous for its contents of native iron and graphite (Steenstrup 1874, 1875; Larsen & Pedersen 2009; Pedersen *et al*. 2017). The Asuk Member was erupted from at least three different centres on Nuussuaq and two on Disko (Fig. 6) close to the end of the second volcanic episode of the Vaigat Formation.
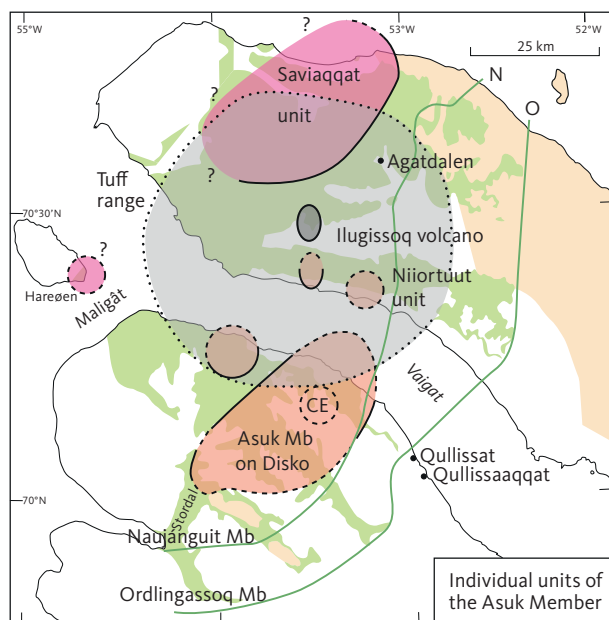
4.2.1.2 The Nunngarut igneous body. The igneous body in the sediments between Qullissat and Qullissaaqqat is here called the Nunngarut igneous body (later: lava flow). It forms an apparently near-horizontal sheet that can be followed along the coast for *c*. 4.7 km with interruptions due to landslides. Where it is in place, its upper boundary is situated just below 300 m altitude (Figs 2 and 3), but neither the upper nor the lower boundary are exposed. The body has recently been investigated by magnetic and multispectral methods, by which a number of more or less slipped blocks were identified beside some stable areas (Jackisch *et al*. 2022). The Nunngarut igneous body is not present north-west of Qullissat and thus occurs about 12 km south-east of the area with lava flows of the Asuk Member. It even occurs south-east of the mapped south-eastern boundary of the entire Vaigat Formation (Figs 1 and 6). Compositionally, the Nunngarut igneous body is a magnesian basaltic andesite with 53–56 wt% SiO_2 and 7.2–8.0 wt% MgO (calculated volatile-free), with highest SiO_2 in the upper part (Olshefsky *et al*. 1995 and analysis from the exposure at Nunngarut in Pedersen *et al*. 2017, table 5). The body is closely similar to the Asuk Member with respect to mineralogy and composition, and it has tentatively been regarded as a sill belonging to the member. The FP94-4-5 core has for the first time allowed us to study the upper and lower contacts of the body.

5 Material and methods

Data for the FP94-4-5 and FP94-4-6 cores are given in Table 1. Also included are data for five short sections (M-1 to Q-3, Figs 2 and 3) measured in the coastal cliffs between Qullissaaqqat and the abandoned coal mine and used here for correlation purposes. Sections Q-1 to Q-3 were published by Pedersen *et al*. (2006).

When the locations of the drill sites given in Olshefsky *et al*. (1995) were checked in the new high-resolution digital elevation model (Styrelsen for Dataforsyning og Infrastruktur 2023), the given altitudes above sea level of 358 and 86 m for holes FP94-4-5 and FP94-4-6,

respectively, did not fit the elevation model and were replaced with our measured altitudes of 315 and 67 m (Table 1). The Universal Transverse Mercator (UTM) coordinates appeared to be correct. Core FP94-4-5 starts at 30.5 m downhole depth and core FP94-4-6 starts at 28.55 m downhole depth because the overlying parts consisted of loose overburden of which no cores are preserved. The cores have a diameter of *c*. 3.6 cm, and they are not slabbed. The preservation state of the rocks is excellent, and the stratification in the laminated sediments appears to be horizontal.

The sedimentological logs show the estimated grain sizes and the sedimentary structures, which form the basis for the identification of sedimentary facies and the interpretation of the depositional environment when combined with the palynological data.

The samples for palynological examination were treated in the lab as described in G.K. Pedersen *et al*. (2023). All palynological slides and (if available) organic residues are stored at GEUS. Total carbon (TC), total organic carbon (TOC) and total sulphur (TS) analyses, Rock-Eval type pyrolysis and vitrinite reflectance measurements were carried out following procedures detailed by Andrews *et al*. (2022). When intervals and metres are mentioned in the core descriptions and discussions, they are downhole depths unless altitudes above sea level (m a.s.l.) are specified.

6 Results

Figure 7 shows overview logs of the two cores in their actual position relative to each other, i.e. relative to the sea level. The Nunngarut igneous body (the drilling target) with 138 m thickness takes up most of the length of core FP94-4-5. The entire sedimentary succession in core FP94-4-6 and the lower part (270–205 m downhole depth) of the sedimentary succession in core FP94-4-5 are interpreted as deltaic deposits of the Atane Formation. Based on the palynological results and the sedimentary facies, the overlying succession in core FP94-4-5 (205–190 m downhole depth)

Table 1 Data for investigated drill cores and surface sections in the Qullissat area.

Core or section	Coordinates		UTM zone 22		Length	Altitudes, m a.s.l.	
	Deg. W	Deg. N	Easting	Northing	m	Top	Bottom
FP94-4-5	53° 00.04′	70° 02.854′	423818	7772428	270.5	315	44.5
FP94-4-6	52° 58.38′	70° 03.147′	424891	7772939	143.26	67	−76.26
Q-1	52° 58.02′	70° 03.236′	425121	7773097	29	29	0
Q-2	52° 58.07′	70° 03.266′	425094	7773152	26	27	1
Q-3	52° 58.32′	70° 03.449′	424931	7773499	53	53	0
M-1	52° 58.95′	70° 03.856′	424568	7774268	27	42	15
M-2	52° 59.12′	70° 03.970′	424469	7774483	22	22	0

Cores: UTM coordinates are as reported in Olshefsky *et al*. (1995); geographical coordinates and altitudes were calculated/measured at GEUS. The cores are stored in GEUS's core repository, Copenhagen. Surface sections Q1 to M2: All coordinates were measured/calculated at GEUS. m a.s.l. = metres above sea level.
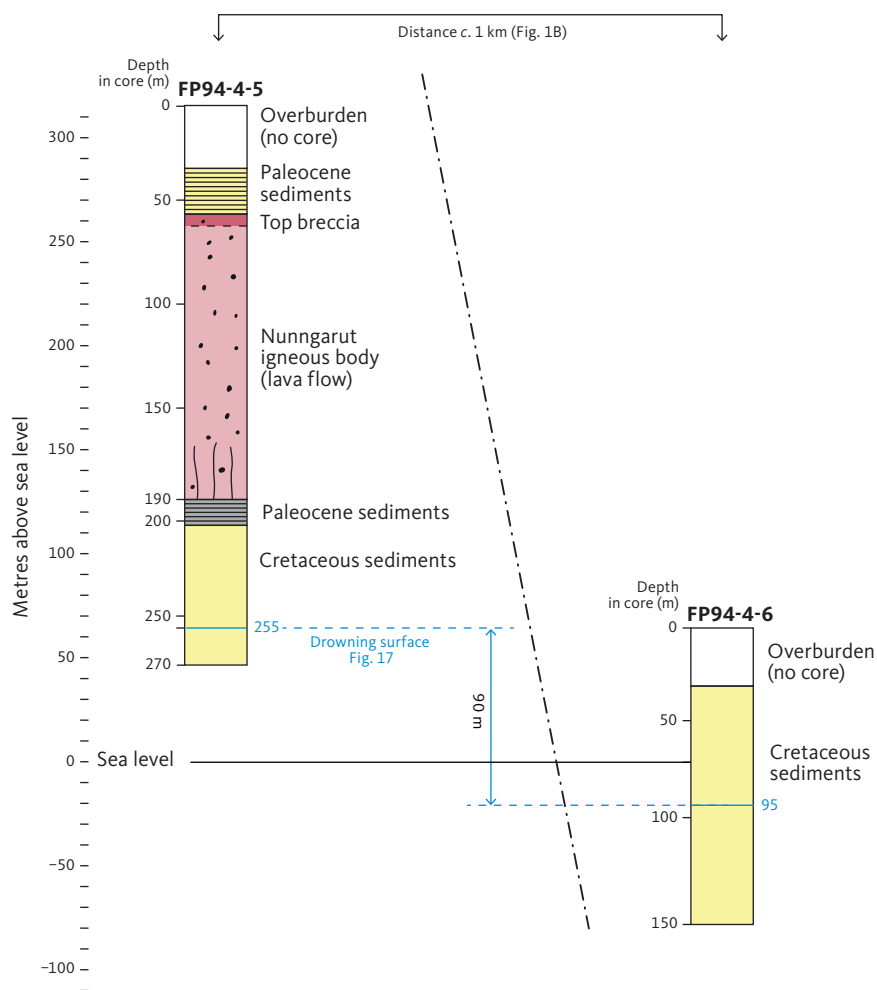
Fig. 7 Simplified overview logs of the investigated cores FP94-4-5 and FP94-4-6 showing their position relative to sea level (scale at left). Downhole depths are shown along each core. Correlation of the Cretaceous sediments in the two cores is based on their sedimentological logs (see below). A characteristic correlatable drowning surface is shown in blue. The surface is situated *c.* 60 m above sea level in core FP94-4-5 and *c.* 30 m below sea level in core FP94-4-6, indicating a vertical displacement between the drill sites of *c.* 90 m along a fault. The fault is schematically indicated on the drawing; its precise position and orientation are uncertain.

is referred to the Paleocene Eqalulik Formation. The sedimentary succession above the Nunngarut igneous body is referred to the Paleocene Atanikerluk Formation.

The horizontal distance between boreholes FP94-4-5 and FP94-4-6 is *c.* 1190 m (Table 1). Vertically, the cores appear to be almost in stratigraphic continuity, as core 5 ends at 45.5 m a.s.l. and core 6 begins at 38.5 m a.s.l. (Fig. 7 and Table 1), and the sediments are near-horizontal. Nonetheless, the sedimentary successions and the biostratigraphy in the two cores may be correlated as shown below, suggesting the presence of a fault between the two core sites (Fig. 7).

6.1 Palynology and ages

A total of 24 samples from FP94-4-5 (GGU no. 393016) and 20 samples from FP94-4-6 (GGU no. 393017) have been processed, and the palynomorphs have been studied. The results are presented in range charts and

photographs of stratigraphically important species in Figs 8–11. The samples are located in the detailed core logs (Fig. 12). Marine dinoflagellate cyst species are common, although their abundances in many samples are low. Several markers (FO: first occurrence and LO: last occurrence of species) also occur in both cores as indicated in the range charts. Some samples containing only spores and pollen probably represent non-marine environments.

6.1.1 Core FP94-4-5

Samples 101 and 108 are barren of dinoflagellate cyst and miospores. Samples 104, 105 and 106 contain a few miospores.

Samples 102 (253 m) and 103 (251 m) contain a few well-preserved specimens of *Heterosphaeridium difficile* and few, not very age-diagnostic dinoflagellate cyst species and the pollen *Rugubivesiculites rugosus*, together indicating an age not older than Turonian.
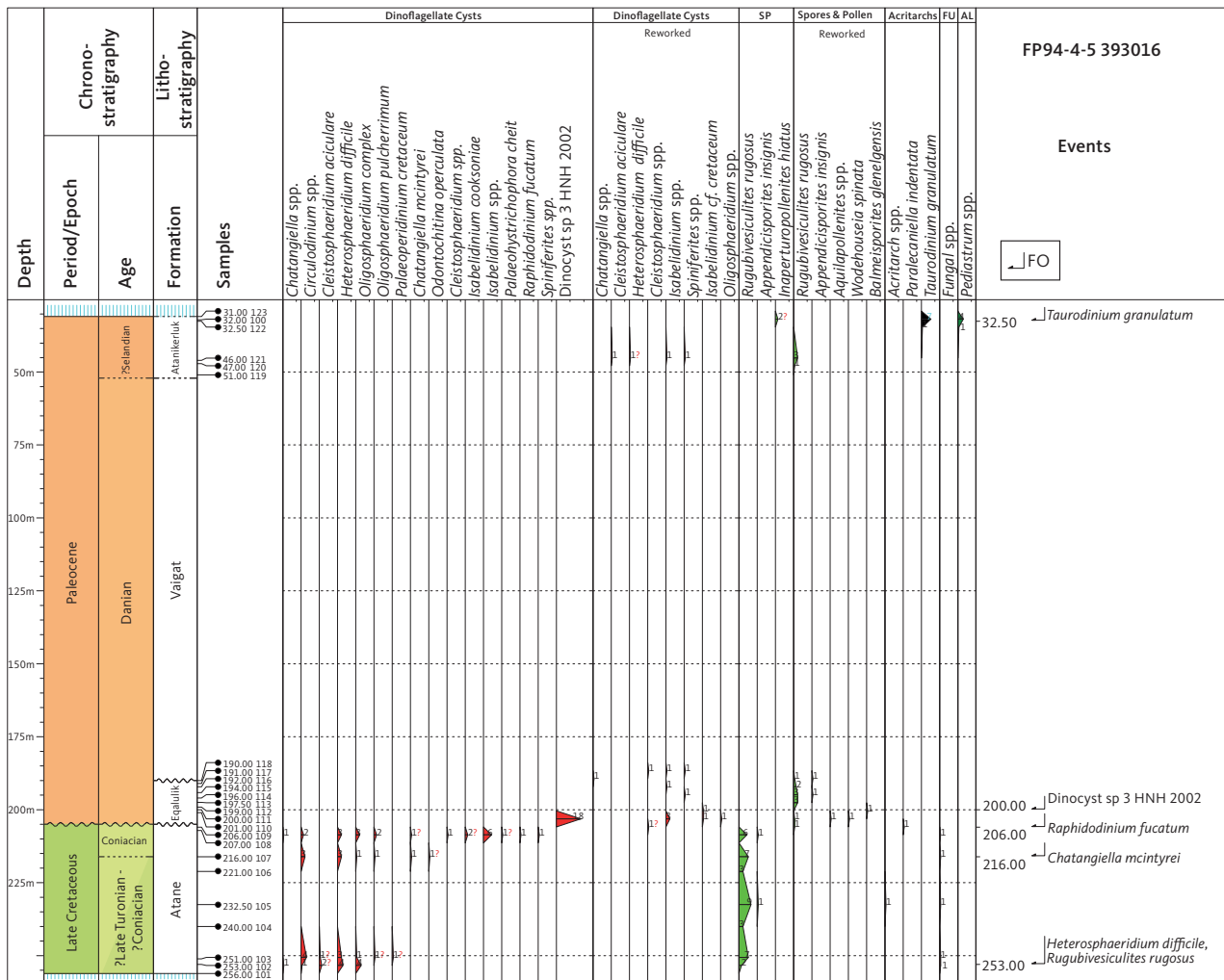
Fig. 8 Range chart of dinoflagellate cysts, spores and pollen (SP), acritarchs, fungi (FU) and freshwater algae (AL) in core FP94-4-5. Biostratigraphically important palyno-events are shown to the right. FO: first occurrence. LO: last occurrence.

Samples 107 (216 m) and 109 (206 m) also contain *Heterosphaeridium difficile* and *Rugubivesiculites rugosus* besides *Isabelidinium* and *Chatangiella* specimens. Sample 109 also contains a poorly preserved *Raphidodinium fucatum* specimen indicating a post middle Turonian age, whereas both samples contain *Chatangiella mcintyrei* which may indicate an early Coniacian age according to Nøhr-Hansen (1996) and Pedersen & Nøhr-Hansen (2014).

Samples 110 (201 m) to 118 (190 m) are of early Paleocene age, possibly Danian. Sample 111 (200 m) contains only one *in situ* dinoflagellate cyst species but a fair number of specimens (18); the species is similar to Dinocyst sp. 3, which was recorded from the Eqalulik Formation on the north coast of Nuussuaq by Nøhr-Hansen *et al*. (2002). Samples 110 (201 m) to 117 (191 m) contain a few reworked upper Cretaceous dinoflagellate cyst specimens (*Isabelidinium/Chatangiella*), the pollen *Rugubivesiculites rugosus* and, in sample 111 (200 m), the Maastrichtian marker pollen species *Wodehouseia spinata*. Sample 118 (190 m, at the contact to the Nunngarut igneous body) only contains coal fragments.

Sample 119 (51 m) contains some small round thick-walled brown bodies. Samples 120 (47 m) and 121 (46 m) contain few reworked upper Cretaceous dinoflagellate cysts and the pollen *Rugubivesiculites rugosus*. Sample 122 (34.2 m) contains three specimens of the dinoflagellate cyst *Taurodinium granulatum* (formerly classified as an acritarch). Sample 100 (32 m; taken before the systematic sampling) contains some *Taurodinium granulatum* and some specimens of the freshwater alga *Pediastrum*. Sample 123 (31 m) contains no dinoflagellate cysts but is dominated by bisaccate pollen.

Piasecki *et al*. (1992) first reported *Taurodinium granulatum* as Gen et sp. indet. from Tuapaat in south-eastern Disko in a sand and mudstone succession in the Rinks Dal Member. Storey *et al*. (1998) dated the Rinks Dal Member to *c*. 61 Ma (Selandian). It is therefore assumed that the presence of the species in samples 122 and 100 represents a Selandian age. For further record of *Taurodinium granulatum*, see Fensome *et al*. (2016, p 72).
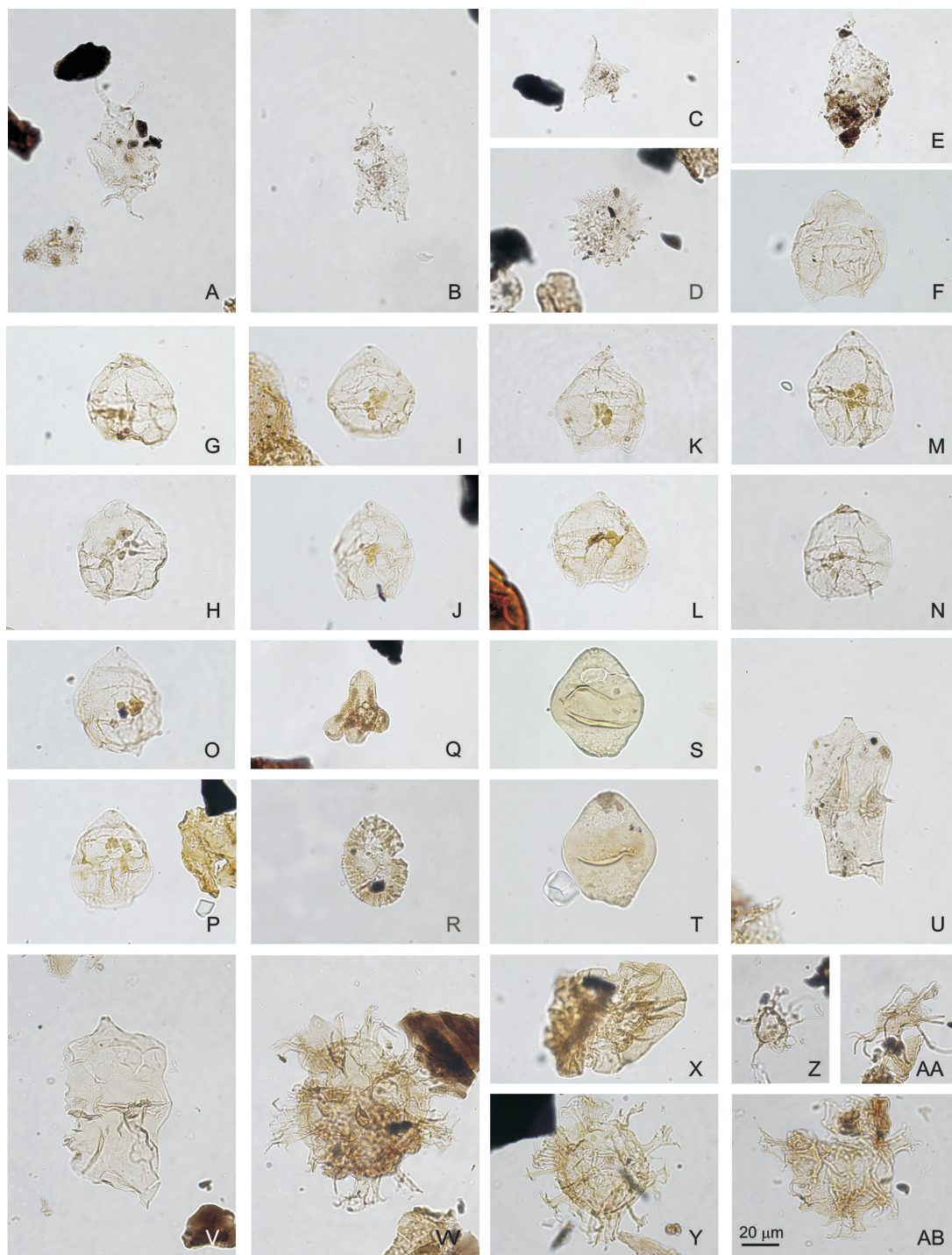
Fig. 9 Palynomorphs from core FP94-4-5. Same magnification for all figures; scale bar in AA = 20 µm. Each figure represents species name, sample no., slide no., England finder coordinate and photo no. **A**: *Taurodinium granulatum*, sample 393016-100, slide 2, W52-3, photo 2709. **B**: *Taurodinium granulatum*, sample 393016-100, slide 3, P28-4, photo 2711. **C**: *Taurodinium granulatum*, sample 393016-100, slide 2, W54-1, photo 2713. **D**: *Pediastrum* sp., sample 393016-100, slide 2, F41-1, photo 2710. **E**: *Taurodinium granulatum*, sample 393016-122, slide 2, H57-1, photo 2708. **F**: Dinocyst sp. 3 Nøhr-Hansen *et al*. (2002), sample 393016-111, slide 6, L19, photo 2582. **G**: Dinocyst sp. 3 Nøhr-Hansen *et al*. (2002), sample 393016-111, slide 6, L30-4, photo 2586. **H**: Dinocyst sp. 3 Nøhr-Hansen *et al*. (2002), sample 393016-111, slide 6, F42-1, photo 2595. **I**: Dinocyst sp. 3 Nøhr-Hansen *et al*. (2002), sample 393016-111, slide 6, Z20-2, photo 2583. **J**: Dinocyst sp. 3 Nøhr-Hansen *et al*. (2002), sample 393016-111, slide 6, W26-2, photo 2585. **K**: Dinocyst sp. 3 Nøhr-Hansen *et al*. (2002), sample 393016-111, slide 6, X38-1, photo 2591. **L**: Dinocyst sp. 3 Nøhr-Hansen *et al*. (2002), sample 393016-111, slide 6, F42-1, photo 2592. **M**: Dinocyst sp. 3 Nøhr-Hansen *et al*. (2002), sample 393016-111, slide 6, X32, photo 2588. **N**: Dinocyst sp. 3 Nøhr-Hansen *et al*. (2002), sample 393016-111, slide 6, P42-2, photo 2699. **O**: Dinocyst sp. 3 Nøhr-Hansen *et al*. (2002), sample 393016-111, slide 6, O42-4, photo 2581. **P**: Dinocyst sp. 3 Nøhr-Hansen *et al*. (2002), sample 393016-111, slide 6, G23-3, photo 2584. **Q**: *Aquilapollenites* sp. reworked, sample 393016-111, slide 4, U31-1, photo 2704. **R**: *Wodehousia* sp. reworked, sample 393016-111, slide 6, H20-4, photo 2701. **S**: *Isabelidinium* cf. *cretaceum* reworked, sample 393016-112, slide 6, X37-4, photo 2706. **T**: *Isabelidinium* cf. *cretaceum* reworked, sample 393016-111, slide 6, S25-4, photo 2702. **U**: *Chatangiella mcintyrei*, reworked, sample 393016-111, slide 6, Q29-1, photo 2700. **V**: *Chatangiella mcintyrei*, sample 393016-107, slide 6, Q21-1, photo 2691. **W**: *Heterosphaeridium difficile*, sample 393016-107, slide 6, L49-1, photo 2693. **X**: *Rugubivesiculites rugosus*, sample 393016-106, slide 5, L46-2, photo 2698. **Y**: *Heterosphaeridium difficile*, sample 393016-102, slide 5, G45-4, photo 2688. **Z**: *Raphidodinium fucatum*, sample 393016-109, slide 6, Q27-4, photo 2697. **AA**: *Raphidodinium fucatum*, sample 393016-109, slide 4, G28-1, photo 2698. **AB**: *Heterosphaeridium difficile*, sample 393016-102, slide 5, X39, photo 2687.
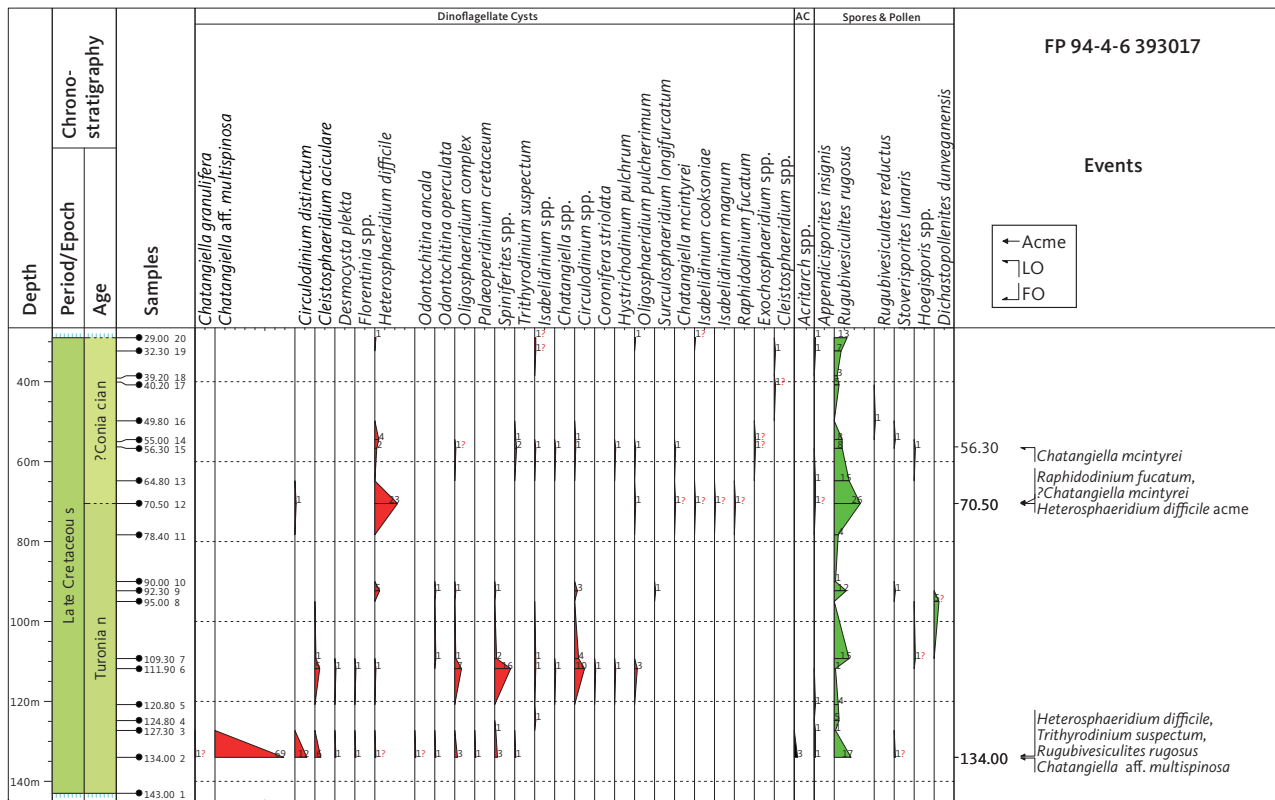
Fig. 10 Range chart of dinoflagellate cysts, spores and pollen, and acritarchs (AC) in core FP94-4-6. Biostratigraphically important palyno-events are shown to the right. FO: first occurrence. LO: last occurrence

In conclusion, the Atane Formation in FP94-4-5 is interpreted to be of late Turonian to Coniacian age. The sediments at 205–201 m are assumed to be Danian, and those at 201–190 m are of Danian age and are referred to the Eqalulik Formation. The sediments above the Nunngarut igneous body at 51–31 m are of Selandian age and are referred to the Atanikerluk Formation.

6.1.2 Core FP94-4-6
Samples 1, 8, 10, 11 and 16 are barren of dinoflagellate cysts, and samples 3, 4, 5, 17 and 18 are nearly so.

Sample 2 (134 m) contains *Trithyrodinium suspectum* (indicating a late Cenomanian or younger age), questionable *Heterosphaeridium difficile* and *Chatangiella granulifera* specimens (indicating a Turonian or younger age). The dinoflagellate cyst assemblage is dominated by a species tentatively described as *Chatangiella* aff. *multispinosa*; the species was originally described from the Albian to Cenomanian of Western Australia by Cookson & Eisenack (1970) and later reported from the Santonian on Antartica as *Chatangiella* cf. *multispinosa* by Keating (1992).

The species *Heterosphaeridium difficile* is present in five samples from sample 2 (134 m) to sample 20 (29 m), with an acme in sample 12 (70.5 m). The acme of *Heterosphaeridium difficile* together with ?*Raphidodinium fucatum* and ?*Chatangiella mcintyrei* indicates a Coniacian age according to Nøhr-Hansen (1996),

Pedersen & Nøhr-Hansen (2014) and Bailey & BioStrat (2021). The possible last occurrence (LO) of *Chatangiella mcintyrei* at sample 15 (56.3 m) and the presence of *Heterosphaeridium difficile* in the uppermost sample 20 (29 m) indicate a minimum late Coniacian or early Santonian age according to Bailey & BioStrat (2021). The pollen *Rugubivesiculites rugosus* is present in all the 20 studied samples.

In conclusion, the Atane Formation in FP94-4-6 is of Turonian (143–70.5 m) and Coniacian (70.5–29 m) age.

6.1.3 Palynology of coal seams B–C in the coastal cliff at Qullissaaqqat
Palynological samples from coal seams B and C from coastal section Q-3 (see Fig. 17) are all dominated by spores, primarily from ferns but also from bryophytes, while pollen from gymnosperms and angiosperms are rare, the latter two groups making up 7–26% of the spore-pollen content in coal seam B and 9% in coal seam C. This suggests that both coal seams represent relatively open mires that were not dominated by trees or bushes. This differs somewhat from the interpretation made by Pedersen *et al.* (2006), who suggested that trees and large bushed were present in the mire flora, based on the coal petrographic dominance of huminite and occasionally inertinite, but with a slightly higher proportion of herbaceous plants in coal seam C.
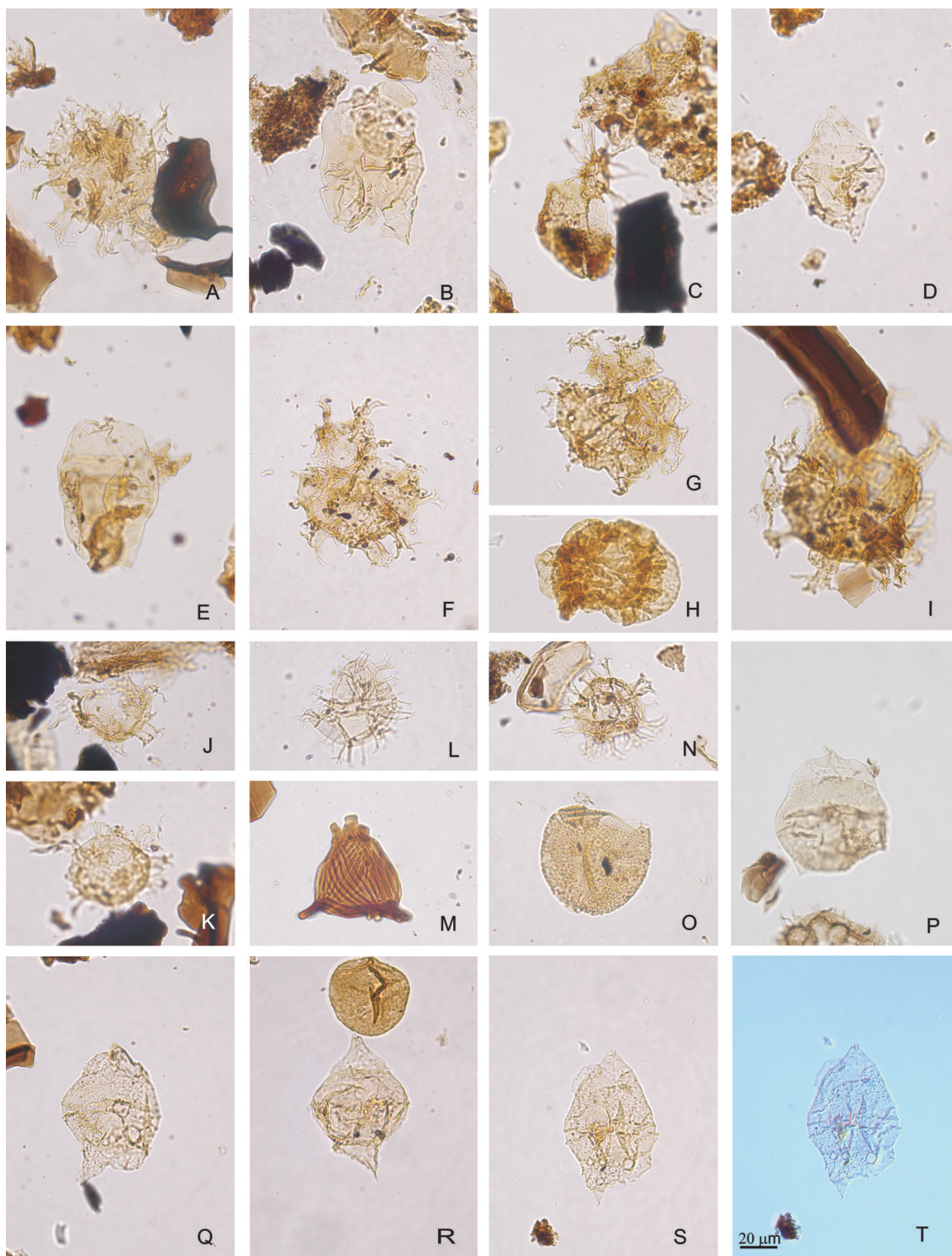
Fig. 11 Palynomorphs from core FP94-4-6. Same magnification for all figures; scale bar in T = 20 µm. Each figure represents species name, sample no., slide no., England finder coordinate and photo no. **A**: *Heterosphaeridium difficile*, sample 393017-15, slide 5, E50-3, Multifocus. **B**: *Chatangiella mcintyrei*, sample 393017-15, slide 4, G48-4, photo 2741. **C**: *Raphidodinium fucatum*, sample 393017-12, slide 4, W34-4, photo 2740. **D**: *Chatangiella mcintyrei*, sample 393017-12, slide 5, S19-1, photo 2739. **E**: *Chatangiella mcintyrei*, sample 393017-12, slide 4, T50-4-1, photo 2738. **F**: *Heterosphaeridium difficile*, sample 393017-12, slide 2, C31-3, photo 2737. **G**: *Heterosphaeridium difficile*, sample 393017-9, slide 5, J22-4, photo 2735. **H**: *Rugubivesiculites rugosus*, sample 393017-9, slide 4, H29-4, photo 2736. **I**: *Heterosphaeridium difficile*, sample 393017-9, slide 5, E53-2, photo 2733. **J**: *Heterosphaeridium difficile*, sample 393017-6, slide 4, A32-1, photo 2732. **K**: *Heterosphaeridium difficile*, sample 393017-6, slide 4, L55-4, photo 2731. **L**: *Spiniferites* sp., sample 393017-6, slide 4, B52-3, photo 2729. **M**: *Appendicisporites insignis*, sample 393017-3, slide 4, W34-1, photo 2728. **N**: *? Heterosphaeridium difficile*, sample 393017-2, slide 4, S34-2, photo 2735. **O**: *Trithyrodinium suspectum*, sample 393017-2, slide 5, C28-3, photo 2724. **P**: *Chatangiella* cf. *granulifera*, sample 393017-2, slide 4, X26-1, photo 2720. **Q**: *Chatangiella* aff. *multispinosa*, sample 393017-2, slide 4, H32.4, photo 2719. **R**: *Chatangiella* aff. *multispinosa*, sample 393017-2, slide 4, Q47-3, photo 2718. **S**: *Chatangiella* aff. *multispinosa*, sample 393017-2, slide 4, P19-2, photo 2716. **T**: *Chatangiella* aff. *multispinosa*, sample 393017-2, slide 4, P19-2, photo 2715.
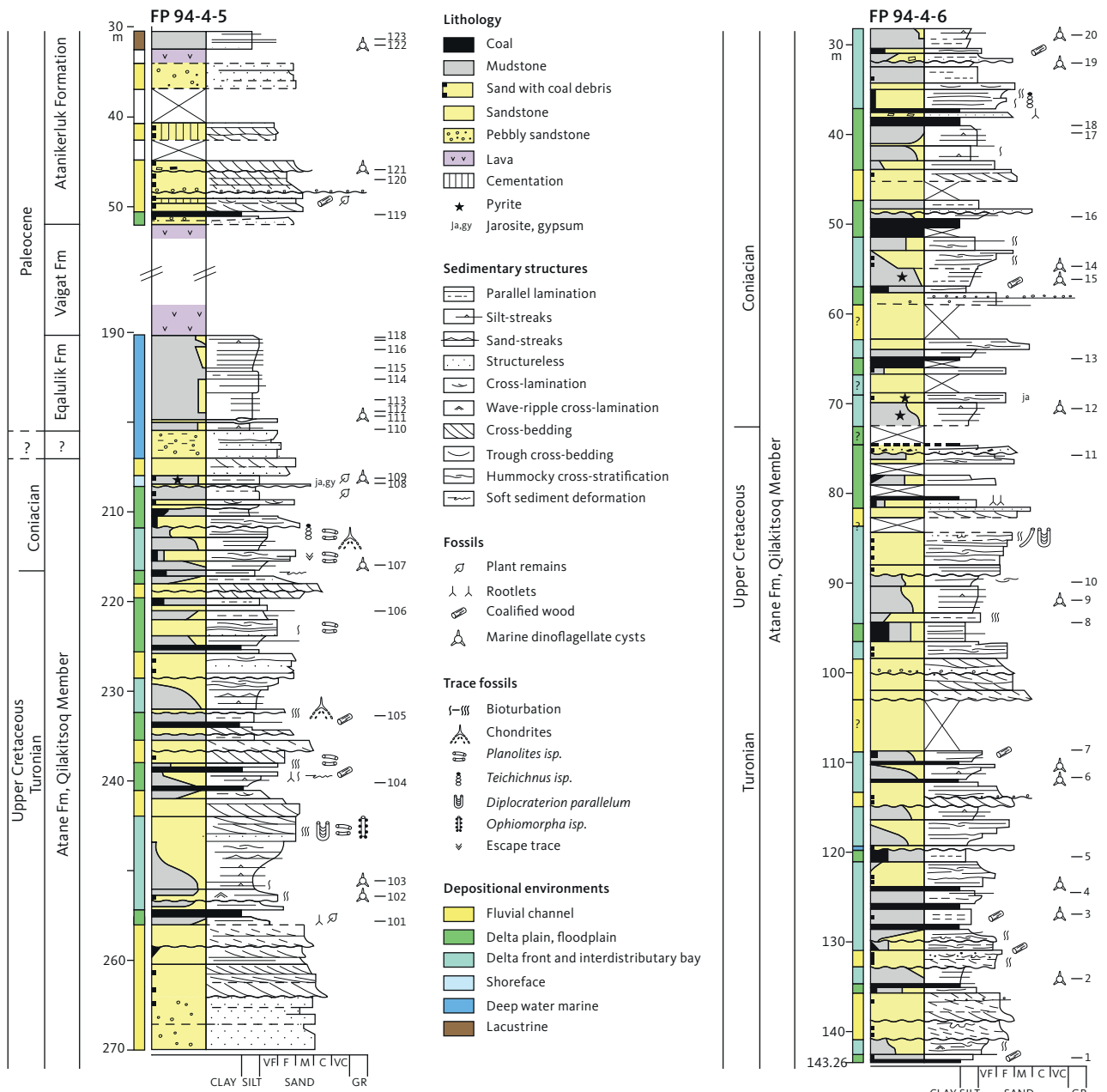
Fig. 12 Sedimentological logs of cores FP94-4-5 and FP94-4-6.

6.2 Vitrinite reflectance and organic geochemistry

Three core samples were analysed for vitrinite reflectance and organic geochemistry: a carbonaceous mudstone 10 cm below the base of the Nunngarut igneous body, a coal seam 2.3 m above the body and a carbonaceous mudstone *c*. 1 m above the body. The last sample is from a short and very broken core from Hole 94-4-4, situated *c*. 2 km north of Hole 94-4-5 (Olshefsky *et al.* 1995). The results are presented in Table 2.

The organic matter in the sample from below the base of the igneous body has a very high vitrinite reflectance (Ro) of 1.67% Ro and a similarly high T_{max} of 600°C. Except for the deep wells GRO#3 and Umiivik-1, these values are far higher than for other investigated samples in the Nuussuaq Basin which have Ro ≤ 0.57% and T_{max} ≤ 450°C (Shekhar *et al*. 1982; Bojesen-Koefoed *et al.* 2001; Pedersen *et al*. 2006). Even in the GRO#3 well, values of 1.67% Ro are only attained at depths of 2000 m, and T_{max} does not exceed 575°C (Bojesen-Koefoed *et al*. 1997). Comparable values are found only in the lower part of the Umiivik-1 core (2–4% Ro and 470–580°C T_{max}), where they are attributed to the heating effect of several thick sill intrusions at this level (Dam *et al*. 1998a).

The organic matter in the two samples above the igneous body has vitrinite reflectances of 0.35% Ro and 0.50% Ro and T_{max} of 414°C and 428°C (Table 2); these values are within the known and normal ranges for

Table 2 Vitrinite reflectance (Ro) and screening data for organic-rich samples below and above the Nunngarut lava flow.

Core	FP94-4-5	FP94-4-4	FP94-4-5
GGU-no of core	393016	393015	393016
Depth in hole (m)	190.4	48.3	50.5
Distance to lava (m)	0.1 (to base)	c. 1 (to top)	2.3 (to top)
Material	Carbonacous mudstone	Carbonaeous mudstone	Coal
Ro (%)	1.67	0.50	0.36
SD	0.14	0.04	0.02
N (no of points)	128	100	100
TOC (wt%)	1.61	6.77	43.54
TC (wt%)	1.84	6.77	45.92
TS (wt%)	0.70	0.13	2.07
Tmax (°C)	600	428	414
S1 (mg HC/g rock)	0.17	0.12	0.65
S2 (mg HC/g rock)	0.90	8.25	51.97
S3 (mg CO_2/g rock)	2.47		20.91
HI	56	122	119
OI	153		48
PI	0.16	0.01	0.01
PC	0.09	0.69	4.37

SD: 1 σ standard deviation. S1: free hydrocarbons (Rock-Eval type pyrolysis). S2: pyrolytic hydrocarbons (Rock-Eval type pyrolysis). S3: CO_2 from Rock-Eval type pyrolysis. HI: Hydrogen Index ((100*S2)/TOC). OI: Oxygen Index ((100*S3)/TOC). PI: Production Index (S1/(S1+S2)). PC: pyrolytic carbon (0.083*(S1+S2)). TOC: total organic carbon. TC: total carbon. TS: total sulphur.

samples from the Nuussuaq Basin stated earlier. These values translate into a maximum burial temperature of 50–80°C (Barker & Pawlewicz 1994), which, allowing for a higher-than-normal geothermal gradient related to volcanic activity, suggests a depth of burial of less than about 2 km. This is, in turn, in keeping with data from the GRO#3 well (Bojesen-Koefoed et al. 1997).

The sediment below the igneous body has obviously been heated by the emplacement of the body. The heating effect reaches 4 m into the sediment, as judged from the slightly increased magnetic susceptibility of the sediment in this interval (Olshefsky et al. 1995, their appendix II), probably caused by re-magnetisation of magnetite grains during the strong heating. The sediments above the body do not show any trace of being heated, and although the sample distances to the body are greater than for the sample below the base, signs of heating of the sediment on the top should be detectable if the body is a sill, as in the Umiivik-1 well. The absence of heating is simply explicable if the body is a lava flow.

6.3 Atane Formation

The sedimentological logs of the two cores (Fig. 12) show a range of sedimentary facies from cross-bedded sandstone, through heterolithic sandstone and sand-streaked mudstone, to mudstone and coal beds, illustrated by core photographs in Fig. 13. They are interpreted as representing four major depositional environments indicated with colour codes in Fig. 12.

6.3.1 Fluvial and distributary channel sandstones

Cross-bedded, medium- to coarse-grained sandstones, locally with comminuted plant debris, and without marine trace fossils, are typically 2–10 m thick (average c. 4 m) and weakly upwards fining (Fig. 12). Examples of these sandstones occur at 141–135 m and 109–98 m in FP94-4-6 and at 256–270 m in FP94-4-5. They are interpreted as deposited in fluvial and distributary channels. The channel sandstones constitute close to one-third of the Atane Formation in the two cores. Thick sandstone units may represent two phases of fluvial deposition (Fig. 12; section Q-3 at 34–25 m, see Fig. 17). Upwards fining sandstones are interpreted as deposited in minor channels. In the slim cores, intervals of weakly cemented sandstone often have low recovery and occur as loose sand in the core boxes. The base of the fluvial sandstones may truncate the top of delta front successions. The fluvial sandstones are typically overlain by delta-plain deposits.

6.3.2 Delta plain deposits

Mudstones with plant debris interbedded with black coal-bearing mudstones of varying thicknesses and thin sandstone beds characterise the delta plain facies association (Fig. 13B, C). The delta plain units are 1–9 m thick (average c. 4 m) and constitute about one-third of the Atane Formation in the two cores. Thin, upwards coarsening units, associated with coal-rich beds, may have formed during mouth-bar progradation in interdistributary bays. Examples of delta plain successions occur at 129–124 m and 96.7–94.6 in FP94-4-6 and 209.8–206.5 m in FP94-4-5. Chemical analyses show that the black mudstones typically contain less than 50% of organic carbon and thus, strictly speaking, are not coal beds (Table 2). Modern analogues for ancient coals are peat-accumulating mires, which have low contents of clastic material and sulphur, and where peat accumulates in beds that are at least 10 m thick. Such conditions occur in floating mires, low-lying mires and raised mires (Haszeldine 1989). Layers of peat are often reduced to 10% of their original thickness during compaction to coal (Ryer & Langer 1980; Ryer 1981). Thick coal beds therefore represent fairly long periods of time and commonly appear to be laterally continuous.

6.3.3 Transgressive shoreface sandstones

Thin beds 0.1–0.5 m thick, of fine- to medium-grained, well-sorted sandstone with an erosive basis and sometimes with marine trace fossils, separate delta plain deposits (below) from delta front deposits (above). The transgressive shoreface sandstones are rare and constitute c. 1%

Fig. 13 Photographs of the Atane Formation sediments in the cores. Core diameter is 36 mm. **A**: Fine- to medium-grained, cross-bedded sandstone, locally with coalified plant debris, interpreted as fluvial or distributary channel facies. Core FP94-4-5, depth *c*. 237.70–237.50 m. **B**: Delta plain facies, dark grey mudstone with lenses or thin layers of coal. Core FP94-4-5, depth *c*. 238.70–238.55 m. **C**: Delta plain mudstone erosively overlain by bioturbated muddy sandstone, interpreted as an interdistributary bay deposit. The boundary represents an initial transgression. Core FP94-4-6, depth *c*. 94.64–94.43 m. The bioturbated facies is overlain by a thick deltafront succession at *c*. 94.05–81.70 m depth, see Fig. 12. **D**: Bioturbated muddy sandstone, close-up of the trace fossil *Taenidium* isp.; the thorough mottling obscures many individual burrows. Core FP94-4-6, depth *c*. 94.5 m (see **C**). **E**: Dark grey mudstone, interpreted as delta front facies. Core FP94-4-6, depth *c*. 49.75–49.60 m. **F**: Sand-streaked mudstone, alternation between thin layers of very fine-grained sand and layers or laminae of silty mudstone, interpreted as delta front facies. Note the scarcity of burrows. Core FP94-4-5, depth *c*. 215.10–214.95 m. **G–H–I**: Delta front facies. Well-sorted, fine-grained sandstone with thin drapes of silt and coalified plant debris. Local precipitation of pyrite. The sandstone has hummocky cross-stratification (**G–I**) and wave-ripple cross-stratification (**G–H**). Trace fossil are scarce, suggesting rapid deposition and possibly marine reworking. Core FP94-4-6, depth *c*. 90.10–86.35 m. Lengths of core pieces are 16–18 cm.

of the Atane Formation in the cores. Examples occur at 48 m and 119 m in FP94-4-6 and at 254 m in FP94-4-5 (Fig. 12). Transgressive sandstone beds mark longer breaks in sediment accumulation: at Qullissaaqqat, such beds are few and thin, which suggests a palaeogeographic position protected from frequent marine reworking.

6.3.4 Delta front deposits

Figure 12 shows that coarsening upwards (CU) successions, up to 11 m thick, occur through the cored interval of the Atane Formation. Most delta front units are thin, on average *c*. 4 m thick, and constitute close to one-third of the Atane Formation in the cores. This facies association ranges from dark grey mudstone and silt-streaked mudstone through interbedded sandstone and mudstone (Fig. 13F) to sandstone with hummocky cross-stratification (Fig. 13 G–I). Comminuted plant debris occurs in

the sandstones. Marine trace fossils are present, but the degree of bioturbation is generally low. Marine dinoflagellate cysts are present in many samples from this facies association, but commonly in low numbers. The CU units are interpreted as deposited during delta front progradation. Thick CU units, such as 94–84 m and 44–39 m in core FP94-4-6, may be correlated laterally (see Fig. 17).

In the Paatuut area (south coast of Nuussuaq), the delta front deposits constitute 35–40% of the Qilakitsoq Member, and the CU units range in thickness from few metres to *c*. 20 m (Dam *et al*. 2009, fig. 46). The thinner CU units in the Qullissaaqqat area suggest that the entire succession here may represent more proximal parts of the delta.

6.4 Eqalulik Formation

The Eqalulik Formation was cored in FP94-4-5 at 205–190 m (Fig. 12). The basal 4 m consists of structureless

Fig. 14 Photographs of the Eqalulik and Atanikerluk Formation sediments in the cores. **A–D**: Eqalulik Formation; **E–G**: Atanikerluk Formation; all from core FP94-4-5, diameters 36 mm. **A**: Structureless sandstone with very small mudstone clasts in a mudstone matrix. Lower part of the Eqalulik Formation, depth *c*. 201.60–201.45 m. **B**: Dark grey mudstone with sharp-based streaks and thin layers of pale, very fine-grained sand and coarse silt. The thickest layers (3–7 mm) are faintly graded. Red-brown colour is due to cementation. Depth *c*. 200.55–200.40 m. **C**: Mudstone facies characterised by thin layers of angular, light grey grains in a mudstone matrix, interpreted as deposited from thin mudflows with sufficient matrix strength to transport the sand- to granule-sized grains. Depth *c*. 198.95–198.80 m. Note the sharp boundary to homogeneous mudstone at *c*. 198.85 m. **D**: Grey, silt-streaked mudstone, marine deep-water deposit, upper part of the Eqalulik Formation, depth *c*. 191.95–191.80 m. **E**: Cross-bedded, grey sandstone with tiny mudstone clasts. Atanikerluk Formation, depth *c*. 48.08–47.95 m. **F**: Cross-bedded, dark grey sandstone with numerous tiny mudstone clasts, depth *c*. 46.45–46.30 m. **G**: Angular and rounded, moderately sorted clasts in a matrix od sand and mud, interpreted as colluvial deposits. Depth *c*. 36.90–36.75 m.

sandstone (Fig. 14A), which probably was deposited during a marine transgression. The homogeneous sandstone facies is overlain by silt-streaked black mudstones (Fig. 14B). The mudstone locally contains thin streaks of sand-sized light grains in the mudstone matrix (Fig. 14C). This texture is tentatively interpreted as deposition from cohesive mudflows in which the matrix strength was sufficient to prevent the coarse sand from settling (Talling *et al*. 2012). The laminated, silt-streaked mudstone (Fig. 14D) is interpreted to have been deposited at some distance from the coastline and at depths well below wave-base, as no indications of wave-reworking have been recognised. Distinct tuff beds have not been recognised in the formation in core FP94-4-5 but are known from other sections (Dam *et al*. 2009). The uppermost mudstone has a baked zone of at least 10 cm thickness at the contact to the overlying Nunngarut igneous body.

6.5 Atanikerluk Formation

The sediment overlying the Nunngarut igneous body at 52.0–50.9 m consists of light grey, irregular, altered volcanic clasts 1–5 mm in size in a weakly bedded, dark violet-grey matrix that contains quartz grains (Figs 15, 16A). There are scattered, small (1–2 mm) black clasts and red-oxidised patches in the matrix. The clast size decreases upwards. At 50.9–50.3 m, the rock is a siltstone heavily crushed by the drilling but including 15 cm massive coal in the middle. This is overlain by cross-bedded sandstone (50.3–35.4 m), 0.3 m drilling-disturbed volcaniclastic sediment with quartz grains, a small intrusion? (33.8–32.6 m) and 2 m of mudstone (32.6–30.5 m). Recovery was moderate above 45 m, and no core was recovered above 30.5 m.

The lower part of the sandstone interval comprises medium-grained, cross-bedded sandstone (50.3–46.2 m, Fig. 14E–F) with some coal debris. It may represent fluvial

deposits. The overlying fine-grained sandstone (46.2–45.3 m) appears to be hummocky cross-stratified suggesting wave-reworking. Two metres of intraformational conglomerate with sand and mudstone clasts in a clayey matrix (37.3–35.4 m, Fig. 14G) may represent mudflow deposits (colluvial deposits). The small intrusion? of fine-grained, aphyric basalt is emplaced between the sandstones and overlying mudstones. It is at least 1.4 m thick, but no contacts are preserved. The mudstones range from dark brown, structureless clay with thin beds of yellow sand to greyish silty mudstone with thin streaks of silt and very fine-grained sand. The occurrence of the dinoflagellate cyst *Taurodinium granulatum* (see section on palynology) suggests near-contemporaneity with the lower part (Rinks Dal Member) of the Maligât Formation (Fig. 4).

6.6 The Nunngarut igneous body

The complete body was penetrated in Hole FP94-4-5 from 52 to 190 m downhole depth, i.e., at *c.* 263–125 m a.s.l. (Fig. 7). It is thus 138 m thick. A detailed log of the top zone is shown in Fig. 15.

The basal contact to the underlying dark mudstone is sharp, with only *c.* 10 cm basal breccia consisting of angular fragments in a brown matrix presumably of altered glass; a white carbonate-silicate mineral vein *c.* 1 cm in thickness cuts the basal zone (Fig. 16J). The solid rock near the contact is very fine-grained but not strongly chilled.

The main rock is relatively uniform in character throughout. It is a massive, fine-grained, grey rock with scattered orthopyroxene phenocrysts 2–5 mm long. The groundmass structure varies from nearly homogeneous over streaky to patchy with intermixed darker and lighter grey patches with bulbous and wispy shapes (Fig. 16G). A detailed study of the mineralogy and chemistry of the body was conducted by Lode *et al*. (2021). The native iron is finely disseminated through the rock and is not visible to the naked eye. Sediment xenoliths up to 4 cm in size occur scattered through the length of the core; they consist of black mudstones and light yellowish sandstones with lobate and digested margins and reaction rims (Fig. 16H–I). The lower *c.* 25 m of the core is broken up by long, vertical fractures.

The top zone is *c.* 6 m thick (58.1–52 m) and is brecciated in a number of intervals with gradual transitions between them (Fig. 15). The lowest zone (58.1–55.6 m) is greenish grey and more or less fragmental; it becomes less compact upwards, and the clasts become more easily visible. Both clasts and matrix are finely vesicular (Fig. 16F). At 55.6–55.4 m, the degree of oxidation increases upwards, and at 55.4–54.0 m, the rock is a striking, red-oxidised volcanic breccia with brick-red to reddish, dark grey to almost black, angular, vesicular clasts of highly variable size up to several centimetres, but most commonly around 1 cm. The matrix is whitish grey and carbonate-rich (Fig. 16E).

At 54.0–53.3 m, the volcanic breccia is grey to brownish grey, with a gradual transition to oxidised clasts in the upper 10 cm. At 53.3–52.8 m, the rock is a red-oxidised volcanic breccia of a character similar to that at the lower level (Fig. 16D). At 52.8–52.0 m, the breccia is greenish grey and compact, with close-lying, irregular, mostly rounded, vesicular clasts up to more than 1 cm in size (Fig. 16C). Scattered orthopyroxene phenocrysts in the breccia clasts show that these consist of a rock similar to that of the massive lava. Around 52 m, the rock has large clasts scattered in a clearly sedimentary matrix (Fig. 16B). There is no sharp boundary between igneous rock and sediment, but we put the top of the igneous body at 52.0 m.

7 Discussion

7.1 Correlation of cores and the existence of a fault between them

It is possible to correlate the major parts of the Atane Formation in cores FP94-4-5 and FP94-4-6 (Fig. 17) and to extend the correlation to five short logs from the coastal cliffs north-west of Qullissaaqqat (Figs 2 and 3 and Table 1). The correlation is primarily based on the sedimentary successions in both cores and is supported by the presence of Coniacian dinoflagellate cysts in both
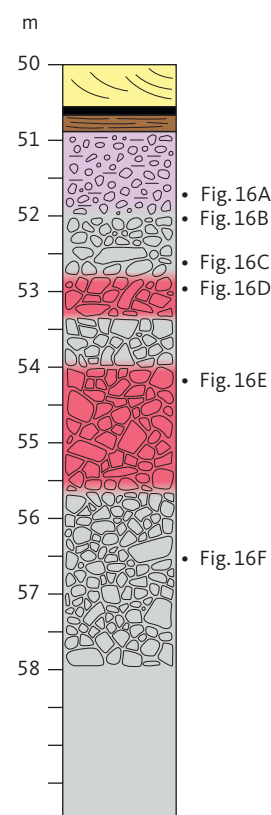

Fig. 15 Detailed log of the brecciated top zone of the Nunngarut igneous body and the overlying sediments. The positions of the photographs in Fig. 16 are indicated.
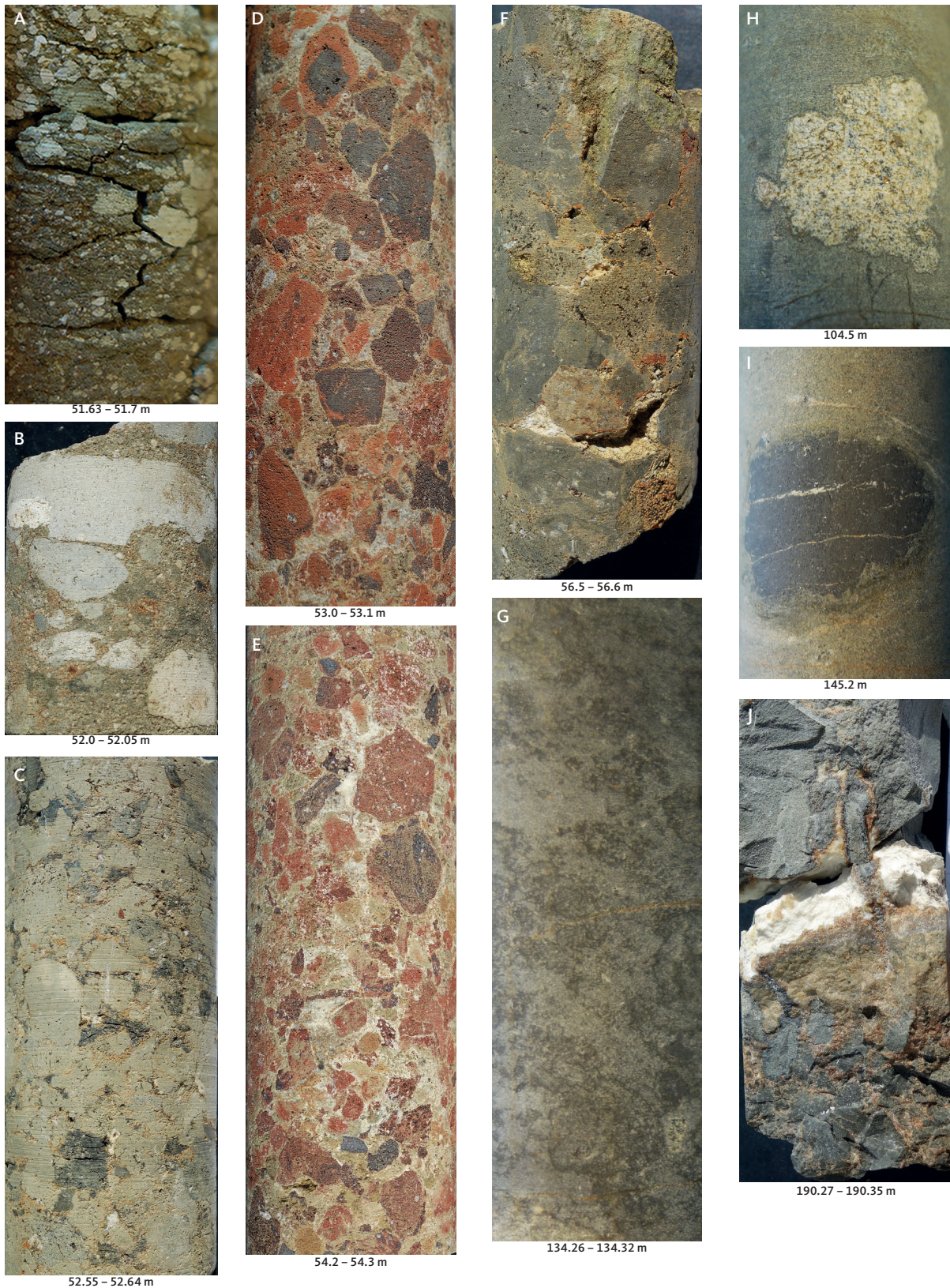
Fig. 16 Photographs of details of the Nunngarut igneous body and immediately overlying sediments. Beneath each piece, the downhole depth is indicated. Positions in the core are shown in Fig. 15. **A**: Sediment (colluvium) with altered volcanic clasts in a weakly bedded matrix. **B**: Large, altered volcanic clasts in a clearly sedimentary matrix, immediately above the top of the igneous body. **C**: Grey volcanic breccia with close-lying, commonly vesiculated, volcanic fragments and little matrix. **D**: Upper red breccia zone of more or less oxidised, volcanic fragments in a light, carbonate-rich matrix. **E**: Lower red breccia zone; note vesiculation in the uppermost, large, angular fragment. **F**: Dark grey, compact volcanic breccia with angular, finely vesiculated clasts. **G**: Inhomogeneous, 'wispy' facies in the central part of the body. **H**: Partly digested sandstone xenolith. **I**: Partly digested mudstone xenolith. Note the homogeneous facies of the host rock surrounding both xenoliths. **J**: The base of the igneous body. The rock is solid above the white vein, and the basal breccia is seen below the vein.
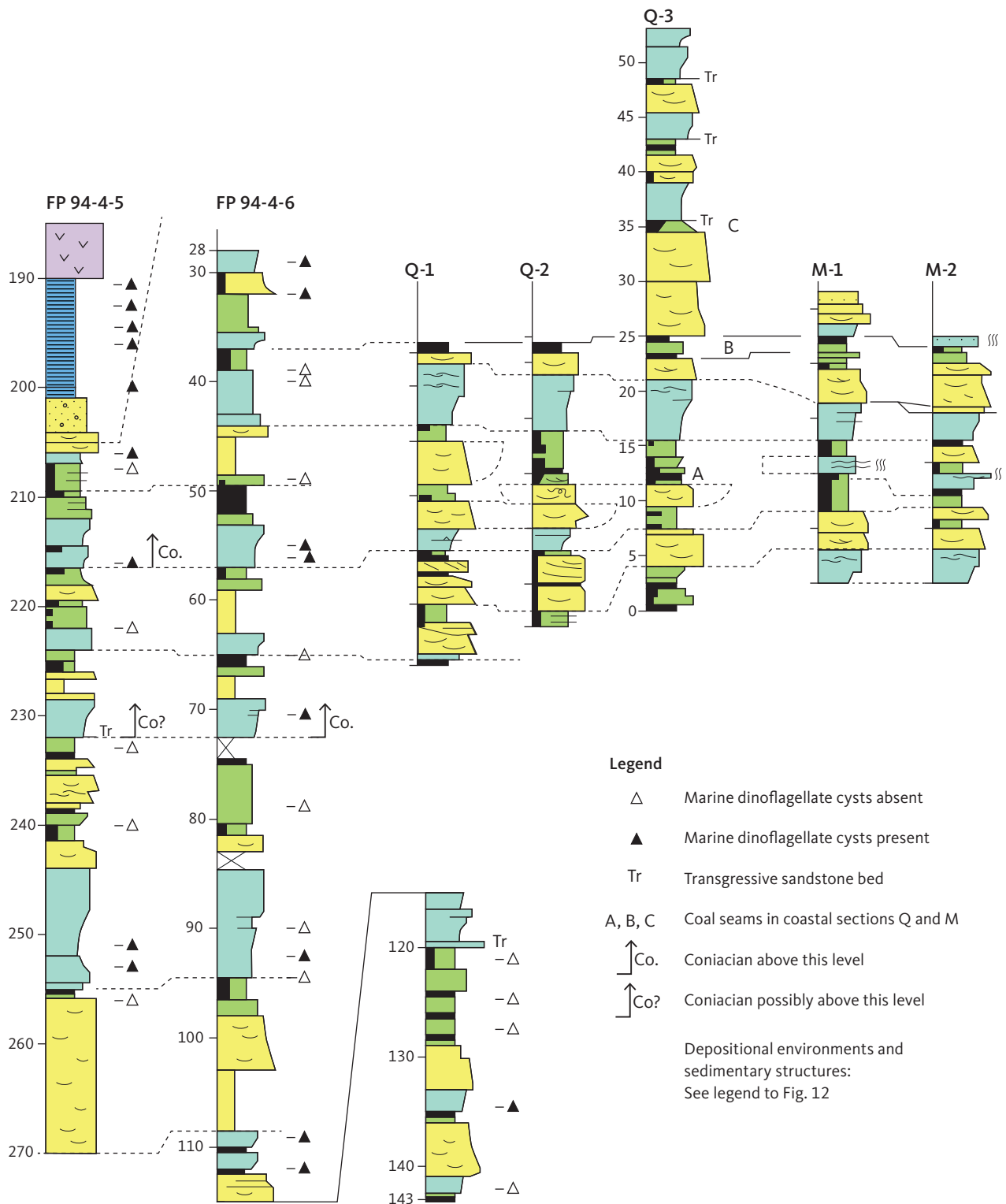
Fig. 17 Correlation diagram of the sedimentary facies associations in the two cores and five surface sections located in Figs 2 and 3.

cores; the Turonian–Coniacian transition is present in core FP94-4-6 and probably present in core FP94-4-5 (Figs 8, 10 and 17).

Correlation of similar successions of the Qilakitsoq Member has shown that the thick coarsening-upwards units are laterally continuous and, thus, are reliable markers for correlation (Dam *et al*. 2009, fig. 46). The sedimentological correlation shows minor variations in

thicknesses and facies, but these are known from previous studies of the formation and agree with studies of similar modern environments.

All seven sections in Fig. 17 include several coal beds. Correlation to the coal layer exploited in the closed mine at the coast some 2 km farther north-west is uncertain due to poor exposures, but it is probably identical to layer B in section Q-3.

The correlation in Fig. 17 conflicts with the present depths of the cores (Fig. 7). The correlation indicates that the strata known from borehole FP94-4-6 and the coastal sections have been displaced approximately 90 m downwards relative to the strata in borehole FP94-4-5. The observed lack of the Coniacian marker species *Chatangiella mcintyrei* in the lower part of FP94-4-5 could perhaps be an effect of the very low density of dinoflagellate cysts in the samples, where a single specimen of *Chatangiella mcintyrei* in a sample could make a difference (Figs 8 and 10). On the balance of the evidence, in particular the mutual consistency of the two independent lines of evidence (facies correlation and palynology), we consider that the strata in core FP-94-4-6 have been displaced *c*. 90 m relative to the succession in core FP94-4-5 (Fig. 7).

The displacement process could have been faulting or landsliding. Large parts of the coastal slopes in this region have repeatedly slipped, and, indeed, borehole FP94-4-5 was placed just outside the headscarp of a large rotational slide seen in Fig. 2. This slide is relatively superficial, and the slide plane is located above the sediments in the coastal cliffs, so that the sediments below the slide plane are not deformed by the sliding (Jackisch *et al*. 2022). However, the downward displacement of the strata in borehole FP94-4-6, and also in the coastal sections, has affected the strata down to at least 76 m below sea level (the bottom of hole FP94-4-6) and has left the sediments on both sides of the displacement plane near-horizontal and apparently undeformed. A very large interglacial landslide with a steep sliding plane could perhaps have caused the movement. A steep fault would also have the required effect. Such a fault must strike roughly NW–SE, which agrees with the NNW–SSE to NW–SE striking faults generated during the Late Rift Phase in the early Campanian to early Maastrichtian (Chalmers *et al*. 1999; Dam *et al*. 2000; Hopper *et al*. 2016, fig. 3.5; Dam & Sønderholm 2021, fig. 5). We consider faulting to be the most likely cause of the displacement.

7.2 Atane Formation

The Atane Formation is largely unknown along the north-east coast of Disko between Asuk and Nuugaarsuk, a stretch of *c*. 60 km (Fig. 1), where exposures are scarce and have not been dated until now. The palynological results from the two cores show that the Atane Formation sediments between Qullissaaqqat and Qullissat are of late Turonian–early Coniacian age and belong to the Qilakitsoq Member (Figs 4, 8 and 10). This result is unexpected because previous examinations of palynomorphs from the Atane Formation in outcrops from Asuk to Kussinerujuk have indicated a late Albian to Cenomanian age (Bojesen-Koefoed *et*

al. 2007; Pedersen & Nøhr-Hansen 2014) and thus the presence of the Kingittoq Member (Fig. 4; Dam *et al*. 2009).

On Nuussuaq, the areal distribution of the Kingittoq and Qilakitsoq Members (Fig. 5) appears to be relatively straightforward: the members occupy separate areas with the Kingittoq Member to the east and the Qilakitsoq Member to the west (probably overlying distal parts of the Kingittoq Member at depth). Both members are exposed up to altitudes of 600–800 m, which indicates that a fault with downthrow to the west is located in the 4-km-wide, unexposed zone between Kingittoq and Paatuut (Figs 1 and 5; A.K. Pedersen *et al*. 2007a,b), as also indicated by, e.g., Chalmers *et al*. (1999) and Hopper *et al*. (2016, fig. 3.5).

On the north coast of Disko, the relation between the Kingittoq and Qilakitsoq Members is probably governed by at least one and possibly more faults that are not exposed. In the well-exposed coastal cliff at Asuk, the strata of the Kingittoq Member dip about 5° eastwards so that the general younging of the succession is towards south-east; a fault located south-east of Qullissaaqqat, with a strike N–S or NE–SW and downthrow to the west, may explain why the coastal cliffs in the Qullissat–Qullissaaqqat area expose the younger Qilakitsoq Mb, whereas farther to the east, the older Skansen Member is exposed. Several faults striking N–S to NE–SW are located in the Vaigat strait, and some of these point directly towards Qullissat and Qullissaaqqat (Chalmers *et al*. 1999; Marcussen *et al*. 2002; Hopper *et al*. 2016). These faults were most probably generated during the Late Rift Phase. In any case, the faulting must be prevolcanic because the overlying volcanic rocks are generally unfaulted. A better constrained structural analysis of the Atane Formation on Disko awaits more age determinations of the undated parts (Fig. 5).

7.3. Eqalulik Formation

The boundary between the Cretaceous Atane Formation and the overlying Danian Eqalulik Formation is located at 205 m in core FP94-4-5 (Fig. 12) and represents a hiatus of *c*. 24 million years (cf. above). The cross-bedded sandstone below 205 m is interpreted as part of the Qilakitsoq Member of the Atane Formation. The medium-grained to fine-grained, structureless sandstone above is interpreted as deposited above a transgressive surface of erosion, formed during the rapid transgression at the base of the Eqalulik Formation (TSS8), discussed by Dam *et al*. (1998b). This transgression is only recorded in some offshore wells (Nøhr-Hansen *et al*. 2002; Fensome *et al*. 2016).

Only a single small exposure of the Eqalulik Formation is known on Disko. In the coastal cliff in the landslide at Asuk, 40 cm of tuffaceous marine mudstone

with dinoflagellate cysts overlies the top of a submarine lava flow and is covered by a subaerial flow, both of the Asuk Member (Piasecki *et al*. 1992; Pedersen *et al*. 2017, fig. 95). The mudstone is a late part of the Eqalulik Formation, whereas the main part must be situated below sea level. A palaeogeographic reconstruction of the marine embayment in which the formation was deposited (Pedersen *et al*. 2017, fig. 136) indicates that it should be present in the Qullissaaqqat area, which is now confirmed. The lack of volcanic material in the core may reflect the long distance to the major volcanic eruption sites in the north-west (Fig. 6) and the general low explosivity of the Vaigat Formation.

The nearest other locality with a complete section through the Eqalulik Formation is exposed at Ataata Kuua on Nuussuaq, 30 km due north of Qullissaaqqat.

7.4 The Nunngarut lava flow

The strongly red-oxidised top breccia of the body shows that the magma has been exposed to open air; it is, thus, not a sill but a lava flow. The two grey-and-red intervals in the top breccia show that the semi-consolidated top crust has been broken up in slabs that were stacked during the final flowage of the magma. Very similar lava flows with stacked and tumbled slabs of crust on the top are described from the Deccan Province by Kale *et al*. (2022).

At the base of the flow, the sediment has been strongly heated, as shown by the high vitrinite reflectance (Table 2). The long, vertical fractures in the lower *c*. 25 m of the core are interpreted as columnar jointing, indicating that the lower part of the flow interacted with water.

The conclusion that the mineralised body is not a sill but a lava flow reduces its economic potential according to the Noril'sk mineralisation model (Lightfoot & Hawkesworth 1997) because the magma throughflow during lava emplacement is expected to be limited. However, its thickness, distribution and volume will still be of interest for future exploration, and the Nunngarut flow is significantly thicker than any other flow or sill known from Disko and Nuussuaq. Similar iron-bearing magnesian basaltic-andesite flows from the Asuk Member have thicknesses up to 45 m at Asuk and 60 m in the Kuugannguaq valley (Pedersen 1985, fig. 9; Pedersen *et al*. 2017, figs 94 and 98). A dacite flow from the Nordfjord Member of the Maligât Formation is 120 m thick (Pedersen *et al*. 2018, fig. 104C). The thickest flows of basaltic composition on Disko and Nuussuaq are 60–80 m thick; these are commonly flows that have run into water-filled depressions and become ponded there.

As the Nuungarut flow is only exposed in a coastal section of *c*. 4.7 km length, its extent (present as well as original) cannot be known. The flow most probably extends to the west beneath the high mountain ridge where it cannot be traced (Fig. 3; Jackisch *et al*. 2022). On the other side of the mountain ridge, flows of the Asuk Member are exposed in both sides of the Kuugannguaq valley. In this valley, the main area with Asuk Member reaches its south-easternmost limit 20 km due west of Qullissaaqqat (Fig. 6). From southern Kuugannguaq, the south-east limit of the member runs north-east beneath the mountain ridge and reappears in the landslipped areas south of Asuk, 12 km north-west of the Nunngarut flow at Qullissat (Fig. 6). In Kuugannguaq and at Asuk, there are iron- and graphite-bearing flows with compositions very similar to that of the Nunngarut flow, in particular 'composite lava 1' in Kuugannguaq (Table 3). No direct eruption sites in the form of craters or feeders for the Asuk Member flows are known, but the main production area must be situated centrally within the area of distribution of the Asuk Member on Disko (Fig. 6). If the Nunngarut flow was erupted from the central area, it must have travelled at least 15 km and probably closer to 20–25 km to reach Qullissaaqqat.

Alternatively, the Nunngarut flow was produced from a separate eruption site about 20 km east of the main production sites, in an area where no magmas were previously produced; however, this is not likely to lead to so closely similar magma compositions as shown in Table 3. We consider it more likely that the magma was erupted from the main production area and flowed the same distance on the ground, aided by gravity. Long travel distances for such relatively siliceous lava flows are known from the Nordfjord Member of the Maligât Formation in western Disko. Here, the Mellemfjord lava flow is a composite, iron-bearing marker flow with basaltic to andesitic composition that covers an area of 28 by 15 km, i.e. more than 400 km^2. It has a thickness up to 88 m and a volume of more than 14 km^3 and is one of the largest flows in the Nuussuaq Basin (Pedersen 1977; Pedersen & Ulff-Møller 1987; Pedersen *et al*. 2018, pp. 147–151).

The known volume of the Nunngarut flow is approximately 5 km (length) × 2 km (width) × 0.13 km (thickness) = 1.3 km^3. However, including its probable extension beneath the younger volcanics and its long travel distance, it must have a considerably larger volume. Moreover, the close compositional similarity between the Nunngarut flow and the iron-bearing flow in Kuugannguaq suggests the possibility that the two flows were produced during the same eruptional event, and in this case, the erupted magma volume may be the largest in the Asuk Member.

7.4.1 Emplacement of the Nunngarut lava flow

At the time of eruption of the Asuk Member, the lava plateau formed an emergent land area in north-western Disko and western Nuussuaq. In central Disko,

the volcanic rocks were banked up against the emergent Disko Gneiss Ridge. To the east and south-east, the volcanic rocks prograded into a narrowing marine embayment connected to the main sea north of Nuussuaq (Pedersen *et al.* 2017, fig. 136). The eastern shore of this embayment received mud and sand from the Paleocene successor of the large Cretaceous river and delta system, and at the sea floor, the synvolcanic mudstones of the Eqalulik Formation accumulated. The surface of the prevolcanic sediments was irregular. When the Vaigat Formation was erupted, highs with palaeovalleys in the old sediments were locally emergent, for example, at Naajannguit 35 km north-west of Qullissat, where such a valley was filled with subaerial lava flows of the Naujánguit Member of the Vaigat Formation, some of the first lava flows that reached Disko (Pedersen *et al.* 2002).

We envisage that the Nunngarut lava flow was erupted in the main magma production area between Kuugannguaq and the north-east coast of Disko (Fig. 6). In this area, accumulated eruption products could have formed a relatively elevated land area, perhaps even one or more local volcanic edifices. Lavas that flowed to the west and south would cover older subaerial lava flows and eventually reach the Disko Gneiss Ridge, as recorded by Pedersen *et al.* (2005). Lavas that flowed to the east and north-east would enter the sea and become brecciated like the first flow at Asuk (Pedersen *et al.* 2017, fig. 94). Lavas that flowed into shallow water and whose top stayed above the water level would maintain coherence but develop colonnades and entablatures like the second flow at Asuk and the Nunngarut flow. A low in the east-sloping sediment surface could have guided the Nunngarut flow for perhaps as much as 20 km to the south-east and into the sea. A coast-near local basin could provide space for ponding of the flow to create its extraordinary thickness. The flow was not brecciated but attained columnar jointing, and its oxidised surface stayed well above the sea level, at least at the drill site. The ability of the lava flow to reach so far and attain such a thickness, even by ponding, requires that the erupted volume was considerable.

7.5 Atanikerluk Formation

The *c.* 1 m of grey to violet-grey, weakly bedded volcaniclastic sediment with siliciclastic grains overlying the top of the Nunngarut lava flow is interpreted as an outwash/colluvial deposit of altered volcanic material and disintegrated quartzofeldspathic sediment washed onto the weathered lava surface from surrounding exposures. The deposit is considered to be of local extent. The overlying *c.* 20 m of cross-bedded sandstone and subordinate mudstone with thin horizons of organic matter of fluvial and lacustrine origin probably had a more extensive distribution. The sand-dominated lithologies in the FP94-4-5 core, with sparse reworked Cretaceous dinoflagellate cysts and Paleocene spores and pollen, are comparable to those of the Akunneq Member of the lower Atanikerluk Formation, which is exposed in eastern Disko between Nuugaarsuk and Pingu, 36–50 km south-east of Qullissaaqqat. Here, the Akunneq Member has thicknesses of 145–165 m, decreasing westwards, and comprises fluvial sandstones with thin interbedded mudstones (Dam *et al.* 2009, figs 128, 132, 133). The lower part contains reworked Cenomanian pollen and few Paleocene spores and pollen, whereas the upper part contains more Paleocene spores and pollen. We tentatively refer the sediments above the Nunngarut lava flow in core FP94-4-5 to the Akunneq Member; the thickness of 20 m is a result of erosion. The Akunneq Member in eastern Disko is not in contact with the volcanic rocks; however, the member is interpreted to correlate with the lower part of the Naujât Member on Nuussuaq, which, in turn, is coeval with the Ordlingassoq Member of the Vaigat Formation (Dam *et al.* 2009, p. 149), i.e. close in time to but slightly younger than the Nunngarut lava flow.

The sediments overlying the Nunngarut lava flow in FP94-4-5 present a rare glimpse of the Atanikerluk

Table 3 Chemical compositions of the Nunngarut lava flow and a lava flow from the Asuk Member in Kuugannguaq.

	Nunngarut flow[1]	Kuugannguaq[2]
	Depth in core	GGU no.
	89–90 m	176736
Major elements, wt%		
SiO_2	54.94	55.01
TiO_2	1.14	1.11
Al_2O_3	15.30	15.19
FeO*	10.18	9.87
MnO	0.14	0.13
MgO	7.26	7.42
CaO	8.24	8.20
Na_2O	1.73	2.14
K_2O	0.93	0.80
P_2O_5	0.14	0.11
	100.00	100.00
S wt%	1.04	0.91
Trace elements, ppm		
Cr	547	627
Ni	433	435
Co	81	57
Cu	232	329
Zn	19	47
Rb	27	26
Ba	218	231
Sr	186	195
Nb	7	7
Zr	131	136
Y	21	24

Major elements were calculated volatile-free. [1]Analysis from Olshefsky *et al.* (1995). [2]Composite lava 1, 70°6.5′N, 53°41.1′E, 357 m a.s.l. [2]Analysis from Pedersen *et al.* (2017). [2]Photograph in Pedersen *et al.* (2017), fig 98.

Formation in north-eastern Disko, where exposures are very rare. The only other nearby *in situ* exposure of the Atanikerluk Formation sediments occurs 4.5 km north-west of FP94-4-5 at *c.* 700 m altitude (Fig. 1B). These are mudstones tentatively referred to the Assoq Member (upper Atanikerluk Formation) by A.K. Pedersen *et al.* (2018, p. 63) and are time-equivalent to the lower Rinks Dal Member of the Maligât Formation. A complete section through the Atanikerluk Formation in Disko west of Nuugaarsuk is still not known.

8 Conclusions

The Cretaceous sedimentary strata between Qullissat and Qullissaaqqat comprise a succession of delta deposits more than 130 m thick. The dinoflagellate cyst assemblages indicate a late Turonian to early Coniacian age, and the succession is referred to the Qilakitsoq Member of the Atane Formation. This member has not been recorded on Disko before.

The Cretaceous sediment successions in the two drill cores at Qullissaaqqat are mutually correlatable and are further correlatable with five short sections in the coastal cliffs between Qullissaaqqat and Qullissat. Thereby, the coal quarried at Ritenbenk's coal quarry and mined at Qullissat is dated to be of early Coniacian age.

The Atane Formation (Qilakitsoq Member) at Qullissaaqqat is younger than the Atane Formation in both eastern Disko (Skansen Member) and north-western Disko (Kingittoq Member). This structure indicates the presence of one or more hidden faults, including one east of Qullissaaqqat. More precise location of the fault, or faults, requires better knowledge of the ages of the formation over long distances of the north-east coast of Disko.

The range charts (Figs 8 and 10) show that marine dinoflagellate cysts are present in roughly half of the samples from the Atane Formation. This indicates that the cores represent a part of the delta where non-marine and marine depositional environments changed repeatedly. Palynological samples from coal seams B and C from outcrop section Q-3 are all dominated by spores from ferns and bryophytes. This suggests that both coal seams represent relatively open mires. The pollen in the samples may come from trees and bushes on higher elevated areas or the hinterland.

Available vitrinite reflectance data from the area consistently suggest a maximum depth of burial of less than 2 km when allowing for a slightly higher than normal geothermal gradient related to the igneous activity in the region (Bojesen-Koefoed *et al.* 1997, 2001; Pedersen *et al.* 2006).

The Danian Eqalulik Formation in core FP94-4-5 consists of 4 m of sand and 11 m of mudstone, of which at least the upper 10 cm is strongly baked by the overlying lava flow. The presence of the formation is in accordance with the palaeogeographic reconstruction of the marine embayment in which the formation was deposited (Pedersen *et al.* 2017, fig. 136). This is the only section through the Eqalulik Formation known from Disko.

The native-iron-bearing Nunngarut igneous body is a lava flow belonging to the Asuk Member of the Vaigat Formation. The change of status from 'assumed sill' to subaerial lava flow diminishes its economic potential because the magma throughflow in a lava flow is expected to be limited. However, the thickness, distribution and volume of the flow will still be of interest for future exploration. It is the thickest flow known from West Greenland and was most probably erupted in a central eruption area for the Asuk Member between the Kuugannguaq valley and the present north-east coast of Disko. It has run towards south-east over sloping terrain, possibly guided through a surface low, for a distance of perhaps up to 20 km to the sea where it ponded and, at least in the area it was drilled, completely displaced the water so that the red-oxidised top was maintained. The erupted volume must have been much larger than the presently known volume of only 1.3 km^3.

The Atanikerluk Formation in core FP94-4-5 consists of *c.* 1 m of locally derived colluvial material deposited on the weathered lava surface, and at least 21 m of fluvial to lacustrine, sand-dominated deposits referred to the Akunneq Member, which is time-equivalent to the Ordlingassoq Member of the Vaigat Formation. The nearest comparable exposures occur 36 km south-east of Qullissaaqqat, illustrating the extreme scarcity of sediment exposures on the north-east coast of Disko.

Additional information

Author contributions

LML, GKP, AKP: conceptualisation, investigation (geology), writing (lead), editing.
HNH, SL: Investigation (palynology), writing, editing.
JBK: Investigation (vitrinite reflectance, organic geochemistry), writing, editing.
EVS: Investigation (photogrammetry), writing, editing.

Competing interests

The authors declare no competing interests.

Additional files

None.

References

Andrews, S., Vosgerau, H. & Bojesen-Koefoed, J. 2022: The sedimentology and depositional environments of the Bastians Dal and Muslingebjerg formations: evidence for the earliest phases of Jurassic rifting in North-East Greenland. GEUS Bulletin **49**, 8311. *https://doi.org/10.34194/geusb.v49.8311*

Bailey, D. & BioStrat Stratigraphic Consultancy 2021: Late Cretaceous zonation. *http://www.biostrat.org.uk/index.html#*

Barker, C.E. & Pawlewicz, M.J. 1994: Calculation of vitrinite reflectance from thermal histories and peak temperature: a comparison of methods. In: Mukhopadhyay, P.K.A.D. & Dow, W.G. (eds): Vitrinite reflectance as a maturity parameter: applications and limitations. American Chemical Society Symposium Series **570**, 216–229. *https://doi.org/10.1021/bk-1994-0570.ch014*

Bojesen-Koefoed, J.A., Christiansen, F.G., Nytoft, H.P. & Dalhoff, F. 1997: Organic geochemistry and thermal maturity of sediments in the GRO#3 well, Nuussuaq, West Greenland. Danmarks og Grønlands Geologiske Undersøgelse Rapport 1997/143, 18 pp. *https://doi.org/10.22008/gpub/14936*

Bojesen-Koefoed, J.A., Dam, G., Nytoft, H.P., Pedersen, G.K. & Petersen, H.I. 2001: Drowning of a nearshore peat-forming environment, Atane Formation (Cretaceous) at Asuk, West Greenland: sedimentology, organic petrography and geochemistry. Organic Geochemistry **32**, 967–980. *https://doi.org/10.1016/S0146-6380(01)00072-9*

Bojesen-Koefoed, J.A., Bidstrup, T., Christiansen, F.G., Dalhoff, F., Gregersen, U., Nytoft, H.P., Nøhr-Hansen, H. & Pedersen, A.K. 2007: Petroleum seepages at Asuk, Disko, West Greenland: implications for regional petroleum exploration. Journal of Petroleum Geology **30**, 219–236. *https://doi.org/10.1111/j.1747-5457.2007.00219.x*

Chalmers, J.A. & Pulvertaft, T.C.R. 2001: Development of the continental margins of the Labrador Sea: a review. In: Wilson, R.C.L., Whitmarsh, R.B., Taylor, B. & Froitzheim, N. (eds): Non-volcanic rifting of continental margins: a comparison of evidence from land and sea. Geological Society, London, Special Publication **187**, 77–105. *https://doi.org/10.1144/gsl.sp.2001.187.01.05*

Chalmers, J.A., Pulvertaft, T.C.R., Marcussen, C. & Pedersen, A.K. 1999: New insight into the structure of the Nuussuaq Basin, central West Greenland. Marine and Petroleum Geology **16**, 197–224. *https://doi.org/10.1016/S0264-8172(98)00077-4*

Clarke, D.B. & Pedersen, A.K. 1976: Tertiary volcanic province of West Greenland. In: Escher, A. & Watt, W.S. (eds): Geology of Greenland, 364–385. Copenhagen: Geological Survey of Greenland. *https://doi.org/10.22008/gpub/38218*

Cookson, I.C. & Eisenack, A. 1970: Cretaceous microplankton from the Eucla Basin, Western Australia. Proceedings of the Royal Society of Victoria **83**(2), 137–157, plates 10–14.

Dam, G. & Nøhr-Hansen, H. 2001: Mantle plumes and sequence stratigraphy; Late Maastrichtian- Early Paleocene of West Greenland. Bulletin of the Geological Society of Denmark **48**, 189–207. *https://doi.org/10.37570/bgsd-2001-48-11*

Dam, G. & Sønderholm, M. 2021: Tectonostratigraphic evolution, palaeogeography and main petroleum plays of the Nuussuaq Basin: An outcrop analogue for the Cretaceous–Palaeogene rift basins offshore West Greenland. Marine and Petroleum Geology **129**, 105047, 33 pp. *https://doi.org/10.1016/j.marpetgeo.2021.105047*

Dam, G., Nøhr-Hansen, H., Christiansen, F.G., Bojesen-Koefoed, J.A. & Laier, T. 1998a: The oldest marine Cretaceous sediments in West Greenland (Umiivik-1 borehole) – record of the Cenomanian–Turonian Anoxic Event? Geology of Greenland Survey Bulletin **180**, 128–137. *https://doi.org/10.34194/ggub.v180.5096*

Dam, G., Larsen, M. & Sønderholm, M.S. 1998b: Sedimentary response to mantle plumes: implications from Paleocene onshore successions, West and East Greenland. Geology **26**, 207–210. *https://doi.org/10.1130/0091-7613(1998)026<0207:srtmpi>2.3.co;2*

Dam, G., Nøhr-Hansen, H., Pedersen, G.K. & Sønderholm, M.S. 2000: Sedimentary and structural evidence of a new early Campanian rift phase in the Nuussuaq Basin, West Greenland. Cretaceous Research **21**, 127–154. *https://doi.org/10.1006/cres.2000.0202*

Dam, G., Pedersen, G.K., Sønderholm, M.S., Midtgaard, H.H., Larsen, L.M., Nøhr-Hansen, H. & Pedersen, A.K. 2009: Lithostratigraphy of the Cretaceous–Paleocene Nuussuaq Group, Nuussuaq Basin, West Greenland. Geological Survey of Denmark and Greenland Bulletin **19**, 171 pp. *https://doi.org/10.34194/geusb.v19.4886*

Dam, G., Sønderholm, M. & Sørensen, E.V. 2020: Inherited basement canyons: impact on sediment distribution in the North Atlantic. Terra Nova **32**(4), 272-280. *https://doi.org/10.1111/ter.12459*

Fensome, R.A., Nøhr-Hansen, H. & Williams, G.L. 2016: Cretaceous and Cenozoic dinoflagellate cysts and other palynomorphs from the western and eastern margins of the Labrador–Baffin Seaway. Geological Survey of Denmark and Greenland Bulletin **36**, 1-143. *https://doi.org/10.34194/geusb.v36.4397*

Gregersen, U., Hopper, J.R. & Knutz, P.C. 2013: Basin seismic stratigraphy and aspects of prospectivity in the NE Baffin Bay, Northwest Greenland. Marine and Petroleum Geology **46**, 1-18. *https://doi.org/10.1016/j.marpetgeo.2013.05.013*

Gregersen, U., Knutz, P.C., Nøhr-Hansen, H., Sheldon, E. & Hopper, J.R. 2019: Tectonostratigraphy and evolution of the West Greenland continental margin. Bulletin of the Geological Society of Denmark **67**, 1–21. *https://doi.org/10.37570/bgsd-2019-67-01*

Gregersen, U. *et al*. 2022: Stratigraphy of the West Greenland margin. In: Dafoe, L.T. & Bingham-Koslowski, N. (eds): Geological synthesis of Baffin Island (Nunavut) and the Labrador–Baffin Seaway. Geological Survey of Canada Bulletin **608**, 247–309. *https://doi.org/10.4095/321849*

Haszeldine, R.S. 1989: Coal reviewed: depositional controls, modern analogues and ancient climates. Geological Society, London, Special Publications **41**, 289–308. *https://doi.org/10.1144/GSL.SP.1989.041.01.20*

Hopper, J.R., Pedersen, G.K., Sørensen, E., Guarnieri, P., Schovsbo, N.H., Kokfelt, T.F., Hjuler, M.L. & Weng, W.L. 2016: Disko–Nuussuaq: structural mapping and GIS compilation to better define petroleum exploration targets on Disko and Nuussuaq. Danmarks og Grønlands Geologiske Undersøgelse Rapport 2016/47, 119 pp. *https://doi.org/10.22008/gpub/32468*

Jackisch, R. *et al*. 2022: Drone-based magnetic and multispectral surveys to develop a 3D model for mineral exploration at Qullissat, Disko Island, Greenland. Solid Earth **13**, 793–825. *https://doi.org/10.5194/se-13-793-2022*

Kale, V.S., Dole, G., Pillai, S.P., Chatterjee, P. & Bodas, M. 2022: Morphological types in the Deccan Volcanic Province, India: implications for emplacement dynamics of continental flood basalts. Geological Society, London, Special Publications **518**, 341–396. *https://doi.org/10.1144/sp518-2020-246*

Keating, J.M. 1992: Palynology of the Lachman Crags Member, Santa Marta Formation (Upper Cretaceous) of north-west James Ross Island. Antarctic Science **4**(3), 293–304. *https://doi.org/10.1017/S0954102092000452*

Koch, B.E. 1959: Contribution to the stratigraphy of the non-marine Tertiary deposits on the south coast of the Nûgssuaq Peninsula, northwest Greenland, with remarks on the fossil flora. Bulletin Grønlands Geologiske Undersøgelse **22**, 1–100. *https://doi.org/10.34194/bullggu.v22.6555*

Koppelhus, E.B. & Pedersen, G.K. 1993: A palynological and sedimentological study of Cretaceous floodplain deposits of the Atane Formation at Skansen and Igdlunguaq, Disko, West Greenland. Cretaceous Research **14**, 707–734. *https://doi.org/10.1006/cres.1993.104*

Larsen, J.G. & Larsen, L.M. 2022: Lithostratigraphy, geology and geochemistry of the Tertiary volcanic rocks on Svartenhuk Halvø and adjoining areas, West Greenland. GEUS Bulletin **50**, 1–121. *https://doi.org/10.34194/geusb.v50.8295*

Larsen, L.M. & Pedersen, A.K. 2009: Petrology of the Paleocene picrites and flood basalts on Disko and Nuussuaq, West Greenland. Journal of Petrology **50**, 1667–1711. *https://doi.org/10.1093/petrology/egp048*

Larsen, L.M., Pedersen, A.K., Tegner, C., Duncan, R.A., Hald, N. & Larsen, J.G. 2016: Age of tertiary volcanic rocks on the West Greenland continental margin: volcanic evolution and event correlation to other parts of the North Atlantic Igneous Province. Geological Magazine **153**, 487–511. *https://doi.org/10.1017/S0016756815000515*

Lightfoot, P.C. & Hawkesworth, C.J. 1997: Flood basalts and magmatic Ni, Cu, and PGE sulphide mineralization; comparative geochemistry of the Noril'sk (Siberian Traps) and West Greenland sequences. In:

Mahoney, J.J. & Coffin, M.L. (eds): Large igneous provinces. Geophysical Monograph **100**, 357–380. Washington, D.C.: American Geophysical Union. *https://doi.org/10.1029/gm100p0357*

Lode, S., Heincke, B. & Keulen, N.T. 2021: Compilation of data acquired by optical microscopy and automated quantitative mineralogy combined with scanning electron microscopy (AQM-SEM) of thin sections from the Qullissat bore hole FP94-4-5 and correlation to petrophysical measurements. Unpublished GEUS Report, 117 pp. *https://doi.org/10.22008/gpub/38174*

Marcussen, C., Skaarup, N. & Chalmers, J.A. 2002: EFP project NuussuaqSeis 2000 – final report. Structure and hydrocarbon potential of the Nuussuaq Basin: acquisition and interpretation of high-resolution multichannel seismic data. Danmarks og Grønlands Geologiske Undersøgelse Rapport 2002/33, 71 pp. *https://doi.org/10.22008/gpub/18438*

Midtgaard, H. 1996: Sedimentology and sequence stratigraphy of coal-bearing synrift sediments on Nuussuaq and Upernivik Ø (U. Albian – L. Cenomanian), central West Greenland. Unpublished PhD thesis, University of Copenhagen, Denmark, 175 pp.

Nøhr-Hansen, H. 1996: Upper Cretaceous dinoflagellate cyst stratigraphy, onshore West Greenland. Bulletin Grønlands Geologiske Undersøgelse **170**, 104 pp. + plates. *https://doi.org/10.34194/bullggu.v170.6730*

Nøhr-Hansen, H., Sheldon, E. & Dam, G. 2002: A new biostratigraphic scheme for the Paleocene onshore West Greenland and its implications for the timing of the pre-volcanic evolution. In: Jolley, D.W. & Bell, B.R. (eds): The North Atlantic Igneous Province: stratigraphy, tectonic, volcanic and magmatic processes. Geological Society, London. Special Publication **197**, 111–156. *https://doi.org/10.1144/gsl.sp.2002.197.01.06*

Nøhr-Hansen, H., Williams, G. & Fensome, R.A. 2016: Biostratigraphic correlation of the western and eastern margins of the Labrador–Baffin Seaway and implications for the regional geology. Geological Survey of Denmark and Greenland Bulletin **37**, 73 pp + appendices. *https://doi.org/10.34194/geusb.v37.4356*

Nøhr-Hansen, H., Pedersen, G.K., Knutz, P.C., Bojesen-Koefoed, J., Śliwińska, K.K., Hovikoski, J., Ineson, J.R., Kristensen, L. & Therkelsen, J. 2021: The Cretaceous succession of northeast Baffin Bay: stratigraphy, sedimentology and petroleum potential. Marine and Petroleum Geology **133**, 45 pp. *https://doi.org/10.1016/j.marpetgeo.2021.105108*

Olsen, T. 1993: Large fluvial systems: the Atane Formation, a fluvio-deltaic example from the Upper Cretaceous of central West Greenland. Sedimentary Geology **85**, 457–473. *https://doi.org/10.1016/0037-0738(93)90098-P*

Olshefsky, K. & Jerome, M. 1994: Falconbridge Greenland A/S, West Greenland Tertiary basalt province. Report on 1993 exploration activities for Prospecting licence # 156 and Exploration licences 02/91 and 03/91, 71 pp + appendices. Unpublished company report, released, GEUS report File no 21356.

Olshefsky, K., Jerome, M., Graves, M., Evans-Lamswood, D. 1995: Falconbridge Greenland A/S, West Greenland Tertiary basalt province. Report on 1994 exploration activities for Prospecting licence 06/94 and Exploration licences 02/91 and 03/91, 65 pp + appendices. Unpublished company report, released, GEUS report File no 21410.

Pedersen, A.K. 1977: Tertiary volcanic geology of the Mellemfjord area, south-west Disko. Rapport Grønlands Geologiske Undersøgelse **81**, 35–51. *https://doi.org/10.34194/rapggu.v81.7512*

Pedersen, A.K. 1985: Lithostratigraphy of the Tertiary Vaigat Formation on Disko, central West Greenland. Rapport Grønlands Geologiske Undersøgelse **124**, 1–30. *https://doi.org/10.34194/rapggu.v124.7879*

Pedersen, A.K. & Larsen, L.M. 2006: The Ilugissoq graphite andesite volcano, central Nuussuaq, West Greenland. Lithos **92**, 1–19. *https://doi.org/10.1016/j.lithos.2006.03.027*

Pedersen, A.K. & Ulff-Møller, F. 1987: Geological Map of Greenland, 1:100 000, Mellemfjord 69 V.1 Nord. Copenhagen: Geological Survey of Denmark and Greenland. *https://doi.org/10.22008/FK2/7CKYD6*

Pedersen, A.K., Larsen, L.M. & Pedersen, G.K. 1996: Filling and plugging of a marine basin by volcanic rocks: the Tunoqqu Member of the Lower Tertiary Vaigat Formation on Nuussuaq, central West Greenland. Bulletin Grønlands Geologiske Undersøgelse **171**, 5–28. *https://doi.org/10.34194/bullggu.v171.6731*

Pedersen, A.K., Larsen, L.M., Riisager, P. & Dueholm, K.S. 2002: Rates of volcanic deposition, facies changes and movements in a dynamic basin: the Nuussuaq Basin, West Greenland, around the C27n–C26r transition. In: Jolley, D.W. & Bell, B.R. (eds): The North Atlantic Igneous Province: stratigraphy, tectonics, volcanic and magmatic processes. Special Publication, Geological Society, London **197**, 157–181. *https://doi.org/10.1144/gsl.sp.2002.197.01.07*

Pedersen, A.K., Larsen, L.M., Pedersen, G.K. & Dueholm, K.S. 2005: Geological section across north central Disko from Nordfjord to Pingu, central West Greenland. 1:20 000 coloured geological sheet. Copenhagen: Geological Survey of Denmark and Greenland. *https://doi.org/10.22008/FK2/SDHFT3*

Pedersen, A.K., Pedersen, G.K., Larsen, L.M., Pulvertaft. T.C.R., Sønderholm, M., & Dueholm, K.S. 2007a: Geological map of the south-east coast of Nuussuaq between Ataata Kuua and Saqqaqdalen, central West Greenland, 1:50 000, with detailed sections. Copenhagen: Geological Survey of Denmark and Greenland. *https://doi.org/10.22008/FK2/V9AHQN*

Pedersen, A.K., Pedersen, G.K., Larsen, L.M., Pulvertaft. T.C.R., Sønderholm, M., & Dueholm, K.S. 2007b: Geological map of the Nuussuaq Basin in southern Nuussuaq, 1:100 000, special map Paatuut, with detailed sections. Copenhagen: Geological Survey of Denmark and Greenland. *https://doi.org/10.22008/FK2/KE1GCB*

Pedersen, A.K., Larsen, L.M. & Pedersen, G.K. 2017: Lithostratigraphy, geology and geochemistry of the volcanic rocks of the Vaigat Formation on Disko and Nuussuaq, Paleocene of West Greenland. Geological Survey of Denmark and Greenland Bulletin **39**, 1–244. *https://doi.org/10.34194/geusb.v39.4354*

Pedersen, A.K., Larsen, L.M. & Pedersen, G.K. 2018: Lithostratigraphy, geology and geochemistry of the volcanic rocks of the Maligât Formation and associated intrusions on Disko and Nuussuaq, Paleocene of West Greenland. Geological Survey of Denmark and Greenland Bulletin **40**, 1–239. *https://doi.org/10.34194/geusb.v40.4326*

Pedersen, G.K. & Nøhr-Hansen, H. 2014: Sedimentary successions and palynoevent stratigraphy from the non-marine Lower Cretaceous to the marine Upper Cretaceous of the Nuussuaq Basin, West Greenland. Bulletin of Canadian Petroleum Geology **62**(4), 261–288. *https://doi.org/10.2113/gscpgbull.62.4.261*

Pedersen, G.K. & Pulvertaft, T.C.R. 1992: The non-marine Cretaceous of the West Greenland Basin, onshore West Greenland. Cretaceous Research **13**, 263–272. *https://doi.org/10.1016/0195-6671(92)90002-8*

Pedersen, G.K., Larsen, L.M., Pedersen, A.K. & Hjortkjær, B.F. 1998: The synvolcanic Naajaat lake, Paleocene of West Greenland. Palaeogeography, Palaeoclimatology, Palaeoecology **140**, 271–287. *https://doi.org/10.1016/s0031-0182(98)00034-0*

Pedersen, G.K., Andersen, L.A., Lundsteen, E.B., Petersen, H.I., Bojesen-Koefoed, J.A. & Nytoft, H.P. 2006: Depositional environments, organic maturity and petroleum potential of the Cretaceous coal-bearing Atane Formation at Qullissat, Nuussuaq Basin, West Greenland. Journal of Petroleum Geology **29**, 3–26. *https://doi.org/10.1111/j.1747-5457.2006.00003.x*

Pedersen, G.K., Nøhr-Hansen, H., Bojesen-Koefoed, J., Grube, K.B., Pedersen, S.A.S., Pedersen, A.K., Sørensen, E.V. & Hopper, J. 2023: A new record of the Cenomanian–Turonian transgression preserved in the Ikorfat Fault zone, Nuussuaq Basin, West Greenland. Cretaceous Research **145**, 105481. *https://doi.org/10.1016/j.cretres.2023.105481*

Piasecki, S., Larsen, L.M., Pedersen, A.K. & Pedersen, G.K. 1992: Palynostratigraphy of the Lower Tertiary volcanics and marine clastic sediments in the southern part of the West Greenland Basin: Implications for the timing and duration of the volcanism. Rapport Grønlands Geologiske Undersøgelse **154**, 13–31. *https://doi.org/10.34194/rapggu.v154.8166*

Rosenkrantz, A., Münther, V., Henderson, G., Pedersen, A.K. & Hald, N. 1976: Geological map of Greenland, 1:100 000, Qutdligssat 70 V.1 Syd. København: Grønlands Geologiske Undersøgelse. *https://doi.org/10.22008/FK2/HIEIU2*

Ryer, T.A. 1981: Deltaic coals of the Ferron Sandstone Member of Mancos Shale: Predictive model for Cretaceous coal-bearing strata of Western Interior. The American Association of Petroleum Geologists Bulletin **65**, 2323–2340. *https://doi.org/10.1306/03b59990-16d1-11d7-8645000102c1865d*

Ryer, T.A. & Langer, A.W. 1980: Thickness change involved in the peat-to-coal transformation for a bituminous coal of Cretaceous age in

central Utah. Journal of Sedimentary Research **50**(3), 987–992. *https://doi.org/10.1306/212F7B44-2B24-11D7-8648000102C1865D*

Schiener, E.J. 1976: Coal geology. In: Escher, A. & Watt, W.S. (eds): Geology of Greenland, 507-516. Copenhagen: Geological Survey of Greenland. *https://doi.org/10.22008/gpub/38218*

Shekhar, S.C., Frandsen, N. & Thomsen, E. 1982: Coal on Nûgssuaq, West Greenland. Unpublished report, Geological Survey of Greenland, 82 pp + appendices.

Steenstrup, K.J.V. 1874: Om de kulförende Dannelser på Öen Disko, Hareöen og Syd-Siden af Nûgssuak's Halvöen i Nord-Grönland. Videnskabelige Meddelelser fra den naturhistoriske Forening i Kjöbenhavn for Aaret **1874**, 75–112 + 3 plates.

Steenstrup, K.J.V. 1875: Om de Nordenskiöldske Jærnmasser og om forekomsten af gedigent Jærn i Basalt. Videnskabelige Meddelelser fra den naturhistoriske Forening i Kjöbenhavn for Aaret **1875**, 284–306 + 2 plates.

Steenstrup, K.J.V. 1877: On the non-meteoric origin of the masses of metallic iron in the basalt of Disko in Greenland. Mineralogical Magazine **1**, 143–148. *https://doi.org/10.1180/minmag.1877.005.1.02*

Steenstrup, K.J.V. 1882: Om Forekomsten af Nikkeljern med Widmann-stättenske Figurer i Basalten i Nord-Grønland. Meddelelser om Grønland **4**(3), 113–131.

Steenstrup, K.J.V. 1900: Beretning om en Undersøgelsesrejse til Øen Disko i Sommeren 1898: Meddelelser om Grønland **24**, 249–306 + plates.

Storey, M., Duncan, R.A., Pedersen, A.K., Larsen, L.M. & Larsen, H.C. 1998: ^{40}Ar/^{39}Ar geochronology of the West Greenland Tertiary volcanic province. Earth and Planetary Science Letters **160**, 569–586. *https://doi.org/10.1016/s0012-821x(98)00112-5*

Styrelsen for Dataforsyning og Infrastruktur 2023: Højdemodel Grønland. *https://dataforsyningen.dk/data/4780*

Svennevig, K., Owen, M.J., Citterio, M., Nielsen, T., Rosing, S., Harff, J., Endier, R., Morlighem, M. & Rignot, E. 2023: Holocene gigascale rock avalanches in Vaigat strait, West Greenland – implications for geohazard. Geology. *https//doi.org/10.1130.G51234.1*

Talling, P.J., Masson, D.G., Sumner, E.J. & Malgesini, G. 2012: Subaqueous sediment density flows: depositional processes and deposit types. Sedimentology **59**, 1937–2003. *https://doi.org/10.1111/j.1365-3091.2012.01353.x*